THE $HN_3 + CO_2$ LASER:
AN ANALYTICAL AND EXPERIMENTAL INVESTIGATION

Francis Kenneth Helmsin

NAVAL POSTGRADUATE SCHOOL
Monterey, California

THESIS

The $HN_3 + CO_2$ Laser:

An Analytical and Experimental Investigation

by

Francis Kenneth Helmsin

Thesis Advisor: D. J. Collins

March 1972

The HN_3 + CO_2 Laser:

An Analytical and Experimental Investigation

by

Francis Kenneth Helmsin
Lieutenant, United States Navy
B.S., United States Naval Academy, 1966

Submitted in partial fulfillment of the
requirements for the degree of

MASTER OF SCIENCE IN AERONAUTICAL ENGINEERING

from the

NAVAL POSTGRADUATE SCHOOL
March 1972

ABSTRACT

One of the most important methods of obtaining laser action, both from a technological and scientific viewpoint, is the chemically-pumped laser. The $HN_3 + CO_2$ chemical laser has been modeled and an experimental investigation conducted to determine the existence of laser action. The analytical model has been used to predict the expected population inversion and laser gain for a range of pressures and various additives. The experimental investigation conducted for comparison with the model did not result in laser action. The increase in pressure for the mixtures investigated indicates the occurrence of an explosion. The lack of detection of laser action has been attributed to difficulties with alignment of the optical system and to signal noise associated with the flash circuit.

TABLE OF CONTENTS

I.	INTRODUCTION	8
II.	THEORY OF HYDROGEN AZIDE EXPLOSION	10
III.	ANALYSIS OF HYDROGEN AZIDE EXPLOSION	13
IV.	ANALYSIS OF THE $HN_3 + CO_2$ LASER	23
V.	$HN_3 + CO_2$ LASER PROGRAM	26
VI.	EXPERIMENTAL TECHNIQUES	28
	A. GENERAL DESCRIPTION	28
	B. FLASH EQUIPMENT	29
	C. CHEMICAL AND VACUUM SYSTEM	32
	D. LASER CAVITY	35
	E. RECORDING EQUIPMENT	37
VII.	RESULTS	39
VIII.	CONCLUSIONS AND RECOMMENDATIONS	43
APPENDIX A.	REACTIONS AND RATE CONSTANTS USED IN THE COMPUTER MODEL	60
APPENDIX B.	$HN_3 + CO_2$ LASER PROGRAM	63
COMPUTER OUTPUT		70
BIBLIOGRAPHY		74
INITIAL DISTRIBUTION LIST		77
FORM DD 1473		78

LIST OF TABLES

TABLE

I Amounts of NaN_3 and H_3PO_4 necessary to generate a desired pressure of HN_3 in a one liter system 59

LIST OF ILLUSTRATIONS

Figure

1. Comparison of theoretical and experimental adiabatic temperature for various dilution of HN_3 — 45
2. Schematic of the grouping of energy levels for the vibrational model — 46
3. Resulting gain from dilution of HN_3 with CO_2 — 47
4. Increase in gain resulting from the addition of He to an $HN_3 + CO_2$ mixture. — 48
5. Experimental setup — 49
6. Schematic of the electrical control box — 50
7. Flashlamp discharge circuit — 51
8. Flash energy vs. capacitor voltage — 52
9. Flash lamp trigger circuit — 53
10. Block diagram of charging system — 54
11. Vacuum system — 55
12. HN_3 gas generator — 56
13. Optical system setup one — 57
14. Optical system setup two — 57
15. Oscilloscope trace of output from photo diode (upper) and IR detector with 10.2 filter (lower) — 58
16. Oscilloscope trace of output from photo diode (upper) and IR detector with Irtran II filter (lower) — 58

TABLE OF SYMBOLS

A_{ij}	Einstein Coefficient
B	Rotational constant
C	Speed of light
C_v	Specific heat at constant volume
$E_{thermal}$	Excess energy released by a reaction
h	Planks constant
H	Photon energy
J	Rotational level
K	Boltzman's constant
M	Molecular weight
N_{CO_2}	Total number density (per unit volume) of CO_2
N_{II}	Number density (per unit volume) of CO_2 in Mode II
N_I	Number density (per unit volume) of CO_2 in Mode I
R_i	Reaction rate
T	Translational temperature
X_i	Volume concentration of chemical species
λ_{ii}	Radiative wave length (10.6 microns for CO_2)
μ	Reduced mass

ACKNOWLEDGEMENTS

The author wishes to express his gratitude to Dr. D. J. Collins for his consultation and guidance. I very much appreciate his patience and advice throughout the period of this investigation.

I wish to extend a special note of thanks to Norman E. Leckenby for his technical assistance.

I. INTRODUCTION

The first laser action was observed by Maiman in 1960. Many different laser systems have since been investigated. One of the most promising systems of efficient laser energy is the chemical laser. Since the energy is stored within the laser medium itself, the chemical laser is of technological interest for its simplicity and compactness. The ability of such a laser to provide insight into the distribution of chemical energy in the products of a reaction make it an attractive tool for understanding complex reactions.

The most favorable reactions for the production of laser action are those which are highly exothermic and involve the formation of products in high energy states. Such reactions are most commonly of the branched-chain type. The excited products may be electronically or vibrationally excited. However, they must be in a state sufficiently differing from equilibrium so as to be capable of producing a population inversion either within the products or by energy transfer to an additive.

The latter method has been extensively investigated using carbon dioxide as an additive; and is the process of interest in the Hydrogen Azide-Carbon Dioxide ($HN_3 + CO_2$) laser. The explosive decomposition of HN_3 produces vibrationally excited nitrogen which subsequently, through near resonant energy transfer, produces a population inversion within the vibrational levels of CO_2. The laser action then occurs through stimulated emissions from the asymmetric vibration level (ν_3 level) of CO_2.

In the following sections a detailed description of the reaction mechanisms involved in the $HN_3 + CO_2$ laser will be presented. The explosive decomposition of HN_3 and the resulting laser gain have been analytically modeled to gain an insight into the potential of the laser. In addition, an experimental investigation has been conducted in order to determine the existence of laser action and applicability of the model.

II. THEORY OF HYDROGEN AZIDE EXPLOSION

Hydrogen Azide (HN_3) is an unstable endothermic gas at room temperature. It is known to explode violently even in the absence of oxygen, above certain limits of temperature and pressure. At low pressures, less than 40 mm Hg, it is a relatively stable compound. However, the stoichiometric process by which HN_3 reacts at these pressures is not constant (Ref. 1). This has hampered the investigation and understanding of the mechanisms by which the reaction proceeds.

The generally adopted reaction mechanism of HN_3 is (Refs. 1 - 7):

$$HN_3 \longrightarrow NH + N_2 \qquad (a)$$

$$N_2 + HN_3 \longrightarrow NH + 2N_2 \qquad (b)$$

$$NH + HN_3 \longrightarrow H_2 + 2N_2 \qquad (c)$$

$$NH + HN_3 \longrightarrow NH_2 + N_3 \qquad (d)$$

$$NH_2 + HN_3 \longrightarrow NH_3 + N_3 \qquad (d1)$$

$$2N_3 \longrightarrow 3N_2 \qquad (d2)$$

$$NH + NH \longrightarrow H_2 + N_2 \qquad (e)$$

Domination of reaction (c) results in a violent explosion while reaction (d) leads to a slowing and eventual quenching of the reaction. The rates at which the two mechanisms proceed are a function of the pressure of HN_3, the method of initiation, and the type and quantity of any diluent (Ref. 7).

Initiation of HN_3 by spark discharge and flash photolysis lead to a domination of reaction (c) while slow thermal decomposition follows reaction (d). However, spark discharge and flash photolysis initiation may still result in the quenching of the explosion by reaction (d) if the dilution of HN_3 is sufficiently high.

Several investigators have suggested reaction (c) be divided into reactions:

$$NH + HN_3 \longrightarrow H_2 + 2N_2 \qquad (c)$$

$$NH + HN_3 \longrightarrow H_2N_2 + N_2 \longrightarrow 2NH + N_2 \qquad (c')$$

The presence of H_2N_2 has not been experimentally observed and reaction c' is 5 Kcal $mole^{-1}$ less exothermic than reaction (c). In addition, H_2N_2 is a relatively stable compound. Therefore it is assumed that if the reaction of NH with HN_3 proceeds via a highly excited H_2N_2 particle, it would decompose preferentially into $H_2 + N_2$.

Reaction (b) as a propagation step has not been observed experimentally, however, it has been suggested as the probable mechanism (Refs. 2,3). The vibrational excitation of nitrogen is consistent with the observed lasing action obtained from the reaction of HN_3 when diluted with CO_2 (Refs. 11,12). It is energetically feasible since there is sufficient excess energy from flash photolysis and reaction (c) to produce vibrationally excited N_2 capable of reacting with HN_3 (Ref. 2).

V. G. Voronkov et. al. (Ref. 8) has suggested a totally different reaction mechanism in which the propagation and branching reactions

are interchanged:

$$NH + HN_3 \longrightarrow H_2 + N_2^*$$

$$N_2^* + \beta\ HN_3 \longrightarrow N_2 + \beta HN + \beta N_2$$

N_2^* is vibrationally excited and capable of decomposing β HN_3 colecules. These reactions are plausible; however, A. S. Rozenberg and V. G. Voronkov (Refs. 9, 10) in later publications have followed the generally accepted reaction mechanism. Therefore the possibility of the interchange of these reactions has not been considered.

III. ANALYSIS OF HN_3 EXPLOSION

If the concentration limits and method of initiation are restricted, an analysis of the explosive decomposition of HN_3 is possible. Since an explosion is necessary for lasing to occur and the method of initiation has been chosen as flash photolysis, prediction of the products of the explosion will allow the laser to be modeled.

Provided the dilution of HN_3 is not sufficient to inhibit an explosion, reaction (d) may be neglected since the products of the reaction have not been experimentally observed (Refs. 1, 4). The equations necessary to describe the explosion become:

$$HN_3 \longrightarrow \dot{N}H + N_2^* \qquad (1)$$

$$N_2^* + HN_3 \longrightarrow \dot{N}H + N_2 + N_2' \qquad (2)$$

$$\dot{N}H + HN_3 \longrightarrow H_2 + 2N_2^* \qquad (3)$$

$$NH + NH \longrightarrow H_2 + N_2' \qquad (4)$$

$$N_2' + M \longrightarrow N_2 + M \qquad (5)$$

$$dT/dt = f(\text{time}, \Delta E) \qquad (6)$$

* N_2 in its ninth vibrational level or higher

' N_2 in less than its ninth vibrational level

· NH in its $a'\Delta$ electronic state

These reactions are divided into sections according to their number so the assumptions and calculations necessary to the model may be stated in detail.

(1) $HN_3 \xrightarrow{-h\nu} \dot{N}H + N_2^*$

Photochemical decomposition of HN_3 was first investigated by Beckman and Dickerson who showed the quantum yield to be 3.0 ± 0.5 and independent of pressure between 2 and 130 mm. of mercury. Flash photolysis of HN_3 has been studied by Cornell, Berry, and Lwowski (Ref. 13) and Thrush (Ref. 4). They detected the presence of the NH radical and identified it in its ground electronic state. Okabe's (Ref. 3) and Welge's (Refs. 14, 15) recent investigations of vacuum-uv photolysis have shown the primary photochemical process in the dissociation of HN_3 to result in N_2 and NH in their $X' \sum_g^+$ and ($a'\Delta$ or $X^3\Sigma^-$) states respectively. Okabe also reported that Stuhl (Ref. 16) detected these as the primary states resulting from flash photolysis. Konar et. al. (Ref. 17) has suggested N_2 to be in a vibrationally excited ground electronic state since selection rules preclude both N_2 and NH from being electronically excited.

It is assumed that NH is formed in its $a'\Delta$ state, having a total energy of 61 Kcal. $mole^{-1}$. For an average quantum wave length of 2125°A the total energy available for dissociation is 154 Kcal. $mole^{-1}$, thus leaving an average of 93 Kcal. $mole^{-1}$ to be shared between the vibrational states of NH and N_2. The principle of equal parittion of energy indicates that nitrogen should be in its ninth vibrational level, thus having an excess energy of 60 Kcal. $mole^{-1}$, more than sufficient for decomposition of HN_3. The remaining 13 Kcal. are assumed to be absorbed as translational energy.

The rate constant for the photolysis of HN_3 may be calculated if the absorption coefficient, quantum yield and energy of the flash is known. The rate of decomposition of HN_3 depends on the photon flux from the flashlamp, its absorption coefficient and the quantum yield and is given by (Ref. 18):

$$R_{HN_3} = \overline{KHV}\,[HN_3] = \phi\,(1 - e^{-\alpha \ell})\,Q$$

where ϕ is photon flux, Q the quantum yield, α the absorption coefficient, ℓ the optical thickness of the absorber and $\overline{KHV}$ the average rate constant.

The average photon flux may be calculated from:

$$\phi = \frac{E_o \xi \Delta\nu_{HN_3} G}{\Delta t\, h\nu_{HN_3}\, \Delta\nu_{fl}}$$

where: E_o is the energy stored in the capacitor bank

ξ	the efficiency of the flashlamp
Δt	pulse duration
$\Delta\nu_{fl}$	flash spectral range
$\Delta\nu_{HN_3}$	absorption band of HN_3
ν_{HN_3}	center frequency of HN_3 absorption band
h	Planks constant
G	geometrical relation between the laser tube and flashlamp

For a discharge energy of 1000j the ILC 7L24 lamp has an efficiency of 85% over the range $\Delta\nu_{fl}$ = 2000°A to 4 microns. The absorption coefficient of HN_3 is 25 at one atmosphere and a center band frequency

of ν_{HN_3} = 2125°A. The absorption band ($\Delta\nu_{HN_3}$) of HN_3 is between 2000°A and 2250°A. The quantum yield is 2.0 (Ref. 5). The geometrical relation between the flashlamp and laser tube is based on the product of the angle which the laser tube subtends on the flashlamp and the reflector coupling of the cavity mirrors. The angle subtended by the laser tube utilized in this inveatigation was 0.2 of the total flash angle and the reflector coupling factor was assumed to be 2.5 (Ref. 19). These values yield a photon flux of: $\phi = 5.4 \times 10^{23}$ photons/sec.

The average rate constant for the decomposition of HN_3 may be calculated from the rate equation:

$$\overline{KHV} = \phi\,(1 - e^{-\alpha l})\; Q/[HN_3]$$

α is independent of pressure, and the average concentration of HN_3 in the laser tube has been taken as 10^{18} particles/cc. Substitution of the above quantities into the equation yield an average rate constant of 3.23×10^{2} sec^{-1}.

From the experimental flash profile the rate of decomposition of HN_3 as a function of time may be determined. This profile is shown in Figure 15 and may best be described by a cubic equation:

$$KHV = at^3 + bt^2 + ct + D$$

From the average rate constant and the experimental profile the boundary conditions on the above equation become:

$t = 0$ $\qquad$ $KHV = 0$

$t = 100$ usec., $\qquad$ $KHV = 0$

$t = 37.5$ usec., $\qquad$ $\frac{dKHV}{dt} = 0$

$$\frac{1}{t}\int_{t=0}^{t=100} KHV\,dt = \overline{KHV}$$

The above boundary conditions yield a rate constant of

$KHV = 2.89 \times 10^{15} t^3 - 6.4 \times 10^{11} t^2 + 3.42 \times 10^{7} t$ where t is in seconds. This rate constant results in total decomposition of HN_3 at a pressure of 6 torr. When 25 torr of HN_3 that is sufficiently diluted to prevent an explosion, only 9.5% of the HN_3 is decomposed.

(2) $\quad N_2^* + HN_3 \longrightarrow \dot{N}H + N_2 + N_2'$

The reaction of N_2^* and HN_3 as the propagation equation for the branched-chain explosion explains the observed dependence on various diluents and hydrocarbon scavengers (Ref. 2). Inorganic diluents do not significantly reduce the rate of formation of products for volume ratios of diluent to HN_3 less than 10. For ratios greater than 10 they slowly decrease the rate of production of products to a maximum of 30% at dilutions of 100 and greater. Hydrocarbon scavengers however have a marked effect and reduce the rate by 70% for dilution ratios less than 10 (Ref. 2). This suggests that inorganic diluents do not react with the excited NH as do the hydrocarbons. Instead they merely increase the rate of relaxation of the vibrationally excited N_2. Since the vibrational

levels of N_2 below the ninth are not sufficiently excited to react with HN_3, this increase in relaxation rate is reflected in the slowing of reaction (2).

Nitrogen particles in vibrational levels above the ninth have been assumed to be in the ninth level. The number of particles in these levels are negligible at room temperature. At higher temperatures the rate of relaxation to a Boltzman distribution in the lower levels is a minimum of ten times faster than the excitation to levels above the ninth.

The rate constant for the reaction of HN_3 with excited nitrogen has been given by Okabe (Ref. 3) as approximately 10^{11} cm^3 $moles^{-1}$ sec^{-1} at 300°K. In order to obtain the temperature dependence of reaction (2), the activation energy of the reaction has been calculated and the rate is assumed to obey an Arrhenius equation ($K = Ae^{-Ea/RT}$). The constant A may then be determined from the known value of the rate constant at 300K.

The activation energy has been calculated from Simple Collision Theory (Ref. 20). The relative Kinetic energy along the line of centers of the two approaching molecules is given by:

$$E_r = \frac{1}{2\mu} \left[M_a^2 v_a^2 + M_b^2 v_b^2 \right]$$

where: M_i is the mass of reactant i

V_i is the mean molecular velocity of i

μ is the reduced mass

The activation energy is related to the E_r in Simple Collision Theory by:

$$E_a = E_r + \frac{RT}{2}$$

where: T = temperature in °K

R = universal gas constant

The mass of N_2 is 28.01 and HN_3 is 43.0. At a temperature of 300°K the above equations yield an activation energy of 6.42 Kcal/mole. The constant A can then be obtained from the Arrhenius equation at a temperature of 300°K:

$$A = Ke^{Ea/RT} = 7.64 \times 10^{-9} \text{ cm}^3 \text{ part}^{-1} \text{ sec}^{-1}$$

and the rate constant can then be expressed as a function of temperature:

$$K2 = 7.65 \times 10^{-9} e^{-6400/Rt} \text{ cm}^3 \text{ part}^{-1} \text{ sec}^{-1}$$

(3) $\dot{N}H + HN_3 \longrightarrow H_2 + 2N_2^*$

The interaction of $\dot{N}H$ with HN_3 is highly exothermic and involves the formation of several bonds which is indicative of a branched-chain reaction, and the creation of vibrationally excited particles (Ref. 21). Since the energy released in such a reaction is concentrated along the bonds of the products, and with the previous assumption of the principle of equal partition of energy, it is assumed that all the nitrogen formed is in the ninth vibrational level. Hydrogen's vibrational levels are much more widely spaced than those of N_2 and it has no low-lying electronic state which could be excited. The participation of hydrogen as a reactant has not been experimentally observed and therefore it is assumed that if hydrogen is formed in an excited state its energy is quickly dissipated into translational energy.

The rate constant for the reaction of HN_3 with various NH radicals has been determined by Okabe (Ref.3). Assuming all NH formed to be in the $a'\Delta$ state the rate of reaction (3) is 5.5×10^{11} cm^3 $moles^{-1}$ sec^{-1} at 300°K. The temperature dependence of the rate constant for reaction (3) has been determined by the same method as that of reaction (2) and has the value of:

$$K3 = 8.7 \times 10^{-7} \, e^{\frac{-8210}{RT}} \quad \frac{cc}{part.\ sec.}$$

(4) $NH + NH \longrightarrow H_2 + N_2'$

Reaction (4) is relatively slow and may be neglected in the prediction of the explosion characteristic of HN_3 (Ref. 10). It does, however, serve to explain the long lasing time observed from an explosion of HN_3 and CO_2; therefore it is included in the model. The rate constant has been obtained from Reference 33 and is:

$$K4 = 3.6 \times 10^{-12} \, T^{0.55} \, e^{\frac{-1900}{RT}} \quad \frac{cc}{part.\ sec.}$$

(5) $N_2\# + M \longrightarrow N_2 + M$; (# = any vibrationally excited level)

In order to predict the effect of inorganic diluents on the explosion, the collisional deactivation of $N_2\#$ must be included. Reaction (5) is not kinetically correct but merely representative of the process. The actual process may be divided in two parts: collisional relaxation of pure nitrogen and the effects of additives.

The derivation of the multi-quantum level population equation is shown in detail in Reference 22 and will not be repeated here. The only assumption involved in the derivation is that transitions are only

allowed between adjacent quantum levels. The validity of this assumption is supported by the agreement obtained with experimental results (Ref. 22). The general equation for the vibrational relaxation of pure nitrogen is given by:

$$\frac{dN_m}{dt} = -K_{m,m+1}N_m - K_{m,m-1}N_m + K_{m+1,m}N_{m+1} + K_{m-1,m}N_{m-1}$$

where K_{ij} is the transition rate for N_2 to or from the m^{th} vibrational level.

The transition rates for pure nitrogen have been obtained from Reference 24 (translational-vibrational) and Reference 28 (vibrational-vibrational) and are:

$$\text{T-V transitions} = 7.34\times10^{21}T^{-1}e^{(-290.4T^{-1/3}-12.5)} \quad T = 1950$$

$$= 7.34\times10^{21}T^{-1}e^{(-56.7T^{-1/3}-31.2)} \quad T = 1950$$

$$\text{V-V transitions} = 9.65\times10^{3}T^{1/2}$$

where: T is in degrees Kelvin and the rates in sec^{-1}.

The increase in vibrational relaxation of N_2 by diluents depends primarily on how well matched the vibrational levels of the diluents are to those of nitrogen. The process of vibrational energy transfer for molecules having exactly matched levels is extremely efficient, occurring approximately every 400 collisions, while the probability of energy transfer for levels differing greater than 200 cm^{-1} may be assumed negligible for most reactions (Ref. 22).

The ν_3 level of carbon dioxide (CO_2) and the ν_1 level of nitrogen differ by only 18 cm^{-1} and therefore an extremely efficient near-resonant energy transfer occurs between these levels. The effect on the explosion by CO_2 and additional diluents of interest to the HN_3 laser are shown in Figure 1.

(6) TEMPERATURE AS A FUNCTION OF TIME

The final quantity necessary for prediction of the products of the explosive decomposition of HN_3 is the variation of the translational temperature with time. In a constant volume system this increase in temperature is due primarily to the energy evolved from the reaction into the translational and rotational motion. Since the relaxation of the rotational levels of a molecule are characteristically on the order of nano-seconds, the energy liberated into rotational energy may be considered as a direct increase in the translational temperature (Refs. 23, 24).

The equation for the raise in translational temperature as a function of time may then be expressed as:

$$\frac{dT}{dt} = \frac{\sum E_{thermal} R_i}{\sum Cv\,[Xi]}$$

The above reactions have been programmed and numerically integrated on the IBM 360 computer. The resultant temperature from the explosion has been compared with the experimental results of A. S. Rosenberg and V. C. Voronkov (Ref. 9) in Figure 1. Exact agreement is not to be expected since the experimental data were obtained from explosions resulting from initiation by a minimum electrical discharge.

IV. ANALYSIS OF THE HN_3 + CO_2 LASER

The extension of the HN_3 explosion model to allow calculation of laser gain may be accomplished relatively easily. The primary equations (effects of diluents on N_2) for the prediction of gain are contained in the explosion model. It is only necessary to consider in greater detail the vibrational relaxation of CO_2 and its energy transfer with the vibrationally excited nitrogen evolved from the explosion.

This vibrational energy transfer process may be described by dividing the vibrationally excited levels of CO_2 into three modes (Ref. 25). As shown in Figure 2, mode 0 contains only CO_2 molecules in their ground vibrational level, mode I those in the symmetric and bending levels, and mode II being those in the asymmetric stretching level.

The energy of the asymmetric stretching level (mode II) of CO_2, as previously noted, is near resonant with the v_1 level of N_2, therefore resulting in a quantum energy transfer approximately every 465 collisions (Ref. 25). In addition, N_2 in its ground electronic state has a zero permanent dipole moment and cannot decay to its ground vibrational level through electric-dipole radiation. Its first vibrational level is metastable, thus being ideal for the selective excitation of the asymmetric stretching level of CO_2.

The V_3 level of CO_2 is also metastable, having (at 420°K and a total pressure of 15 torr) a radiative lifetime on the order to four seconds

and a collisional de-excition rate of 4×10^{-2} seconds (Ref. 25). The levels of mode I at the same conditions have an overall relaxation time of approximately 20 μ-seconds, being limited primarily by the (01'0) level (the lowest vibrational level of CO_2) which required 18 μ-seconds for deactivation. This large difference in relaxation times allows the inversion mechanism by which lasing action may be obtained.

The mechanism of stimulated emission (lasing action) in the CO_2 molecule is characterized by transitions between two vibrational levels. The upper level in CO_2 is the asymmetric stretching level (001) while the lower level is the symmetric level (100). The symmetry of carbon dioxide allows only odd rotational levels in the upper vibrational level and only even in the lower level (Ref. 26). Laser transitions occur between particular rotational levels within the vibrational levels, and correspond to a rotational quantum change of $J=\pm 1$. Changes of $J=+1$ are P-branch transitions and result in a higher gain than those of $J=-1$ which are R-branch transitions. Since lasing action occurs first from the rotational level of the highest gain which is subsequently fed by other levels to maintain a Boltzman distribution (requiring less than 10^{-7} sec.), R-branch transitions do not occur (Ref. 27). This results in a laser emission at a wavelength of 10.6 microns.

In order to calculate the energy output from the $HN_3 + CO_2$ laser, the number of molecules in each vibrational level of CO_2 must be known as a function of time. However, since the vibrational levels of CO_2 greater than (00°1) have an extremely fast relaxation time (200 n-sec at

420°K and 15 torr) and the relaxation of the lower level (100) is limited by the depopulation of the (010) level to the ground state, the population inversion and gain may be calculated within 5% from the knowledge of the total number of molecules within modes I and II (Ref. 25). Considering the assumptions made in prediction of the products of the explosion this is sufficient accuracy. The equations for the population inversion and gain are:

$$PV = (N_{\text{mode II}} - N_{\text{mode I}})/N_{CO_2}$$

$$G_o = \frac{h}{8\pi K}\sqrt{\frac{MC^2}{2\pi K}}\ \frac{\lambda_{21}^3}{T^{3/2}}\ A_{21}(2J+1)B(N_{II}-N_I)e^{-(BJ(J+1)\frac{hc}{KT})}$$

where: PV = population inversion

G_o = gain

Other symbols have their usual quantum mechanical meaning and are listed in the TABLE OF SYMBOLS.

The reactions and rate constants which must be added to the explosion model to determine the above quantities are given in Appendix A. The kinetic rate equations have been numerically integrated using Fortran IV language on the USNPGS IBM 360 computer. A parameter variation based on the above assumptions has been carried out and the results plotted in Figures 3 and 4. These will be discussed in the Results section.

V. $HN_3 + CO_2$ LASER PROGRAM

Equations 1-6 (Appendix A) result in a set of first order linear differential equations. These equations may be integrated to determine the products as a function of time if the rate constants and initial concentrations of the reactants are specified. This integration has been carried out numerically on the USNPGS IBM 360 computer.

The program and a sample output is shown in Appendix B. The relation between computer and usual notation is contained on comment cards within the program. A region of 100K and an average computer time of five minutes is required to predict laser gain.

The USNPGS RKLDEQ library subroutine, employing a Runge-Kutta-Gill predictor-corrector method, has been used to numerically integrate the rate equations. In addition, a variable step size based on temperature has been provided to reduce computer time. Integration is accomplished on a particle per cubic centimeter basis and double precision accuracy (16 significant digits) has been employed to minimize mathematical error.

Data output is controlled by numerically recording every tenth step while laser gain and population inversion are graphically displayed every step once the gain becomes greater than 10^{-5}. The subroutine OSPLOT has been used for plotting gain and population inversion. It

allows an unlimited number of points to be plotted and requires only 0.2 seconds of computer time to plot an average of 200 points.

The sample program in Appendix B is capable of calculating laser gain, population inversion, and vibrational temperature for the $HN_3 + CO_2$ laser with additional diluents of helium, nitrogen or hydrogen. Lasing action and cavity losses have not been considered in the model. If investigation of other inorganic diluents is desired, it may be accomplished by setting He (Helium) in the program equal to the diluents concentration and changing the rate constants specified in the program, to those of the diluent of interest.

The results obtained (Appendix B) allow determination of affects of pressure and diluent variation on the laser gain and population inversion. The assumptions necessary to model the explosion are the limiting factors to the accuracy of the results. Experimental determination of the rate constants for reactions 2 and 3 would resolve this limitation. Experimental observation of laser action would also aid in determination of the quantitative accuracy of the model.

VI. EXPERIMENTAL TECHNIQUES

A chemical laser requires the integration of several very different systems. These apparatus may be divided into five categories: (a) general description; (b) flash equipment; (c) chemical and vacuum systems; (d) laser cavity; (e) recording equipment. This allows a more detailed description of each system and its function in a chemical laser.

A. GENERAL DESCRIPTION

A general block diagram of the laser components is shown in Figure 5. The flashlamp, laser cavity and toxic gas systems are located in a fume hood due to the toxic and explosive nature of the chemicals involved in the generation of HN_3. The fume hood is exhausted to the atmosphere by a fan and has been fitted with a plexiglass covered extension for greater ease in weighing chemicals.

To the left of the fume hood is the main control panel and the remainder of the gas system containing non-toxic, non-reactive gases. All systems can be operated from the main panel with the exception of charging the circuit capacitor bank. In addition, all recording equipment is located in this area for greater safety. On the right is the trigger circuit, electrical control box, capacitor bank, and the charging circuit for the flash system.

Considering the high voltages involved in the flash equipment and the explosive nature of the chemicals, the two systems have been

separated wherever possible. During all experiments the operator is located in area to the left of the fume hood to minimize contact with the high voltage systems. The extension to the fume hood is fitted with rubber seals and in combination with the exhaust fan provides a sub-atmospheric pressure in the interior insuring an air flow away from the operator. The safety features of each system will be covered in the detailed description of the categories below.

B. FLASH EQUIPMENT

The flash system contains three electrically separated circuits: the discharge circuit, triggering circuit, and charging circuit. The three components are integrated through the electrical control box (Fig. 6) located to the right of the fume hood. The entire flash system can be monitored and fired through the control box. However, an additional firing switch has been installed on the main control panel for greater safety.

The discharge circuit (Fig. 7) is a simple series circuit containing the flashlamp, capacitor bank and inductance coil. These may be varied in accordance with Reference 30 to obtain the desired pulse duration and energy output. The flashlamp parameters specified by the manufacturer determine the bounds within which the system may be operated. The flashlamp is a xenon filled, ILC model 7L24 (60 cm. by 7 mm.), lamp with nickel plated copper electrodes. A lamp with either a natural or synthetic quartz envelope may be used in the circuit as designed.

The former emits light of 2000°A and greater while the latter's emission band starts at 1600°A. The synthetic quartz lamp is particularly useful for decomposition of HN_3 which has an absorption band that rises sharply below 2000°A. However, in order to obtain the full effectiveness from the lamp the laser tube must also be made of synthetic quartz. The 7L24 lamp with either envelope has an impedence factor of 116 and requires a minimum trigger voltage of 25KV for 2.4 micro-seconds.

The other two components of the system are the capacitor bank, consisting of four 7 μf. and two 1.5 μf. high voltage (25KV capability) capacitors in parallel, and a 30.0 μh inductance coil made of 3/8-inch copper tubing consisting of 25 windings 15 cm. in diameter. The components have been silver soldered in series using 3 x 1/4-inch copper bars and 3/8-inch copper tubing. The measured ohmic resistance of the circuit is 0.0013 ohms and can be neglected in the calculation of the operating parameters.

The flash circuit has been designed for a damping factor of 0.8 and a pulse duration of 100 μ-sec, with an energy output of 2000 joules. The lamp may be operated under manufacturer's warranty, with a damping factor of 1.1 to 0.7. This allows a variation of energy output with a minimum increase or decrease in pulse duration. The energy output variation with capacitor bank voltage has been calculated from Reference 30 for the allowable damping factor range. Figure 8 shows the energy output in joules for a given capacitor bank voltage.

The triggering circuit creates an ionized spark streamer between the two electrodes which allows the main discharge to occur. It is external to the flashlamp (Fig. 9) and consists of a Dressen-Branes 300 volt, 70 μa DC power supply, an 8 μf. oil filled capacitor, SCR, and a ILC model T105 trigger transformer with a step-up ratio of 60:1. The circuit is controlled by a relay that is energized by pressing the firing switch. A detailed circuit diagram is shown in Figure 9.

The charging circuit consists of a NJE (New Jersey Electronics) Model HA-51 variable high voltage power supply (0-30kv, 0-10μa) which is connected through a high voltage vacuum switch to the capacitor bank in series with a 3mΩ resistor (Fig. 10). When the charge/dump switch is placed in the charge position, the capacitor bank voltage is monitored on a 20 μa API (Assemble Products, Inc.) meter relay on the electrical control box. The meter is calibrated as a voltmeter and interrupts the charging, by isolating the charging circuit and placing the system in the ready-fire position, when the set voltage is reached. A warning flasher is mounted on the control box and is activated at any time the charge/dump switch is placed in the charge position.

Safety is of prime importance to the flash system. With the exception of the flashlamp, the entire system has been placed on the side of the laboratory away from the operator's position during experiments. The flasher on the electrical control box is automatically activated when charging is initiated. The relay meter which separates the charging system when the desired voltage is reached must be

electrically unslaved after firing before the system may be recharged. Plywood covers have been placed over the capacitor bank, inductance coil and high-voltage switches to minimize the danger of operator contact or possible arcing. As constructed, the system is easily operable while providing maximum operator safety.

C. CHEMICAL AND VACUUM SYSTEMS

The chemical and vacuum systems have been integrated through a manifold mounted directly above the laser cavity in the fume hood (Fig. 11). All components of the toxic gas generator are contained under the fume hood while the inert gases and vacuum pump are external to the fume hood and connected to the manifold by 1/8-inch stainless steel tubing. The minifold consists of stainless steel valves that are operated by solenoids from the main control panel. This allows a fast and easy way to isolate any part of the system.

The toxic/explosive gas generator has been designed primarily for use in the generation of Hydrozoic Acid (HN_3). However, it is capable of being used to generate other chemicals in a gaseous state. The description here will be concerned with the generation of HN_3 since its design was for this purpose.

The gas generator is a 500 ml. pyrex flask (Fig. 12) fitted with a pyrex berrette graduated in cubic millimeters. A relief valve has been provided which opens to exhaust at atmospheric pressure to prevent possible damage from over pressure during generation of HN_3. The

system is connected to the manifold through a 1/4-inch pyrex U-tube by a combination of two ball joints and a flexible connection (bellows). The U-tube provides a convenient way of drying the HN_3 with phosphorus pentoxide before it is introduced into the laser tube.

The generation of HN_3 is accomplished by the following reaction (Ref. 31):

$$NaN_3 + H_3P04 \rightarrow HN_3 \uparrow + NaH_2PO_4$$

Sodium Azide (NaN_3: powdered solid) and phosphoric acid (H_3PO_4: 85% syrupy solution in water) are mixed according to their gram atomic weights to provide the desired amount or pressure of HN_3 for the volume of the generation system. Table I shows the weights necessary to generate HN_3 to pressures of 50mm, based on a one-liter system. If the present one-liter system is changed, the quantities of NaN_3 and H_3PO_4 necessary for generating the desired pressure of HN_3 may be obtained by multiplying the data in Table I by the volume of the system. To generate a larger quantity of HN_3 at the same pressure, the laser tube and pressure gauge may be left open during generation. This increases the volume from one to six and one-half liters.

Sodium azide is weighed and placed in the generation flask through the relief valve assembly and then mixed with Dow Corning 704 diffusion pump fluid (silicone based) DCC (Dow Corning Corp.) by means of a teflon coated magnetic stirrer in the bottom of the flask. The quantity of H_3PO_4 used in the generation of HN_3 is chosen slightly higher than stoichiometric to insure all NaN_3 (explosive and toxic)

is consumed. After the system has been evacuated the H_3PO_4 is introduced into the generation flask by a mechanically operated stopcock. The stopcock is controlled from a switch on the main control panel and rotates from fully open to fully closed in 15 seconds.

A plexiglass covered extension to the fume hood has been constructed to allow greater safety in the weighing and handling of the chemicals (Fig. 5). The extension has been sealed by the use of rubber stripping along the edges. A 14- by 12-inch door on one side allows the operator, wearing a face shield, easy access to all parts of the system while handling the chemicals. The exhaust fan provides an airflow away from the operator, which is exhausted to the atmosphere, to prevent inhalation of toxic HN_3 fumes.

The inert gas system is external to the fume hood and is connected to the manifold by 1/8-inch stainless steel tubing. The gases used in the laser were manufactured by ARC (Air Reduction Co., Inc.) and are supplied in one-liter pyrex flasks at a pressure of 755 mm of mercury. Their guaranteed purity is:

Carbon Dioxide	CO_2	:99.995%
Nitrogen	N_2	:99.999%
Helium	He	:99.9995%

Each gas is introduced into the laser tube by a separate solenoid switch. The quantity and rate of induction is controlled by needle valves located immediately behind the inlets. The pressure in the laser tube is monitored by a stainesss steel bourdon tube guage with a range from 0 to 800 mm of mercury and a precision of 0.1% full scale.

Prior to introducing the laser gas mixture the system is evacuated by a mechanical vacuum pump capable of producing a vacuum of 10^{-3} torr. The system is flushed several times during evacuation with an inert gas (N_2) to insure a minimum of impurities in the laser tube. Once evacuation is complete the desired mixture of HN_3 and additional gases are introduced into the laser tube.

D. LASER AND OPTICAL CAVITY

The laser components are mounted on a one-meter standard optical bench (Figs. 13, 14). The laser tube is connected to the manifold, via a ball and socket joint, by 1/4-inch glass tubing which is sealed to a stainless steel bellows.

The laser tube is made of fused quartz and is 60 cm. long with an inner diameter of 30 mm. The ends of the tube have been cut and ground at a Brewster angle of 56° 40' (for sodium chloride) to minimize reflections. Sodium chloride windows were attached to the ends of the quartz tube by chemically inert silicone based cement.

The optical cavity is formed by two gold-surfaced concaved mirrors one inch in diameter placed 78 cm. apart in gimbal mounts made by Oleo Optical Co. The mirrors have a radius of curvature of ten meters. A 2-mm. hole drilled in the center of one mirror provides an output for the recording equipment and allows easy access to the cavity for alignment.

The amount of energy removed by the 2-mm. hole may be calculated from Gaussion theory and is directly related to the laser beam spot size (Ref. 32). This becomes important when small gains are involved and will be discussed in the results section. For the laser cavity described above, Gaussion theory yields a spot size 6.0 mm. in diameter for a wavelength of 10.6 microns and energy removal of 37%. This applies to the lowest order mode. Higher order modes which exist in the comparatively large diameter laser tube extend further in the transverse direction, thus most of their energy is off the axis of the resonator.

Alignment of the laser cavity and recording equipment is comparatively critical and conditions for stability of the cavity are given below:

$$0 \leq g_1 g_2 \leq 1$$

$$L = R_1 R_2$$

Where

$$g_1 = 1 - \frac{L}{R_1}$$

$$g_2 = 1 - \frac{L}{R_2}$$

L = length of the cavity

R_1 = radius of the mirror

The alignment is accomplished using a commercial He-Ne laser with a continuous output of one milliwatt. The He-Ne laser is placed in line with the laser cavity and its beam is passed through the 2 mm. hole in one of the cavities' mirrors. The mirrors are then adjusted until all

reflections within the cavity pass back through the hole and directly into the He-Ne laser. The limit to the precision of alignment (2×10^{-4} radians) is the smallest adjustment which can be made with the gimbal's micrometers.

E. RECORDING EQUIPMENT

In order to effectively monitor the light output from the laser cavity two detectors were used. This allowed the flashlamp discharge to be recorded by one detector while the other was being used in conjunction with various filters to determine any resulting laser energy. The two detector signals were recorded on a dual beam oscilloscope during each experiment. The position of the two detectors in the experimental setup is shown in Figures 13 and 14.

A photo-diode detector was used to monitor the flashlamp discharge. It provided an effective method of monitoring the lamp pulse duration and relative magnitude for various capacitor bank voltages. In addition, it served as the triggering device for the oscilloscope, thus providing a reference for the second detector.

For detection of laser energy a gold-doped germanium detector was used in conjunction with several filters. The detector is cooled by liquid nitrogen and biased controlled to yield a signal of several millivolts. Its maximum response time is 50 nanoseconds over a range of 1.0 to 10.0 microns. Because of the detectors high sensitivity, a monochromator and several different filters were employed in order to eliminate extraneous light.

A Perkrin-Elmer Grating monochromator (MG-12b) with a blaze angle of 12 microns was used to monitor a specific wavelength of light. It was calibrated with a He-Ne laser and cross-checked with a mercury light. When the doors of the monochromator are fully open (2 mm.), a wavelength band of 0.3 microns was provided to the detector, thus eliminating the requirement of filters to attenuate the light signal.

Two different filters were employed without the monochromator in an effort to determine lasing action that might have occurred in a range not allowed by the monochromator. First, an Irtran II filter which passes light between 2.0 and 12 microns was used. However, due to the amount of light emitted in this range by the flashlamp, the oscilloscope vertical scale deflection was limited to 50 millivolts per cm. This was an order of magnitude greater than the expect laser signal and limited determination of any output. A KBR filter passing light only above 10.2 microns was also employed. It allowed oscilloscope deflection as small as 5 millivolts per cm. but eliminated detection of the 9.4 micron band of CO_2.

A sample output of each recording setup is shown in Figures 15 and 16. The oscilloscope vertical response time is 0.06 μ-seconds and scale deflection settings are shown beside each trace. The minimum detectable response is considered to be five millivolts in all cases, due to radiation noise from the flash circuit discharge.

VII. RESULTS

A. THEORETICAL

The agreement of the computer model with the experimental adiabatic temperature (Fig. 1) obtained in Reference 9 showed maximum difference of 9%. This lends some support to the many assumptions necessary to model the explosion. Since the rate constants for reactions (b and c) had to be calculated from sparse experimental data, the determination of exact rate constant as a function of temperature would considerably strengthen the model.

From the large amount of data obtained from the computer model, three factors are of major interest to the experimental investigation of the laser. First is the magnitude of the laser gain for mixtures of $HN_3 + CO_2$. Second, the duration for which the gain is sufficiently high that it may be experimentally observed. And last, is the effect of the addition of He to the laser mixture. These factors have been graphically displayed in Figures 3 and 4.

Figure 3 shows laser gain as a function of the dilution ratio of CO_2 to HN_3. The ratios for which gain is obtainable is broadened as the pressure of HN_3 is reduced. This is indicative of a total pressure limitation on the laser. For 40 torr of HN_3 and a total pressure of 150 torr the vibrational relaxation rate of CO_2 becomes comparable to the reaction rates of the explosion which precludes laser gain. In addition, the maximum pulse duration occurs at dilution ratios less

than those of maximum gain. The pulse duration falls slowly on either side of the maximum. This becomes important in the experimental observation of laser action only at high pressures where the pulse duration approaches the response time of the experimental recording equipment.

The effects of the addition of He to the laser mixture are quite pronounced. A significant increase in gain as well as pulse duration results. Figure 4 shows increase in gain with dilution of He for 25 torr of HN_3. With 100 torrs He added to the mixture, the gain is more than doubled and the maximum pulse increases from 5 to 26 μsec. Further increases in He results in a slight decrease in gain while the pulse duration remains nearly constant. However, dilutions of greater than 4 to 1 for He is approaching the lower limit of the model where the reactions neglected become important.

From the results of the computer model, it would appear that laser action could be obtained even in the crudest of experimental setups. However, two things have not been considered in modeling the HN_3 + CO_2 laser. The actual particle depletion that results from laser radiation and the possibility of a reaction involving $\dot{N}H$ and CO_2. The addition of the former requires a significant increase in the number of assumptions necessary for modeling the laser and could well degrade the accuracy of the results. The latter would only be speculation since very little is known about the reaction of $\dot{N}H$ with any molecule. The limitations and accuracy of the model are contingent on experimental observation of laser action.

B. EXPERIMENTAL

An experimental investigation of the $HN_3 + CO_2$ laser was conducted for pressures of HN_3 from 6 to 35 torr. In addition to pure CO_2, Helium (He) was also used as a diluent under CO_2 starved conditions in order to maintain a temperature less than 2500°K. Although no laser action was observed, it was confirmed that flash photolysis in excess of 1000J. produced explosive decomposition of HN_3 and resulted in a 100% increase in pressure from HN_3. This result adds some support to the assumptions of the explosion model but does not provide an insight into the reasons for the unobserved laser action.

Of primary importance to laser action is the alignment of the optical cavity. The alignment of the far cavity mirror is certainly within the limits necessary; however, the relatively large diameter hole (2.0 mm.) in the output mirror makes its alighment difficult. In addition the vibrations from the vacuum pump, which was mounted near the laser cavity, adds to the doubt of the necessary accuracy in alignment.

The large amount of energy (37%) extracted by a 2-mm. diameter hole, in addition to the Brewster window and mirror losses (estimated at 2.0%), would preclude laser action if the gain were lower than that predicted by the model. For this reason, two closed mirrors were also used; however, alignment was even more doubtful under this setup since it required alignment on the front of one mirror and the back of the other.

Two additional factors which hampered the detection of laser action were radiation from the triggering circuit and the necessity of storing the laser mixture in the system's only pressure gage. The radiation was on the order of 5 millivolts per centimeter and therefore would only be significant under conditions of small gain. The trigger circuit was redesigned to no avail and finally a pulse generator was ordered; however, delays in delivery prevented its use. The storing of the laser mixture in the pressure gage, however, precluded its use during evacuation of the laser tube after each experiment. The elimination of the products from the laser tube therefore was based on time. However, this is thought to be of minor importance and is easily remedied by the addition of a small pressure sensing device.

The latter problems are of minor importance and correction was only limited by the time required for delivery of the necessary equipment. However, alignment is most critical to the detection of laser action. For this reason it is thought that a beam splitter internal to the resonator cavity should be used for alignment so both mirrors may be closed and aligned at the same time. The most effective method of determination of laser output is that of a gain experiment, and in addition it insures alignment of all components in the system at the same time. The timely repair of the CO_2 laser which was to be used in gain experimentation prevented this type of investigation.

VIII. CONCLUSIONS AND RECOMMENDATIONS

The major objectives of the research conducted were the analytical modeling and experimental determination of laser action for the $HN_3 + CO_2$ chemical laser. The analytical model has been completed in the form of a computer model which predicts the magnitude and duration of laser gain as well as the population inversion within the laser medium. Experimental observation of laser action has not been accomplished; however, the results obtained indicate difficulties in the experimental setup to be the reason.

The following recommendations are made for possible improvements in the model and experimental investigation:

A. ANALYTICAL MODEL

1. Experimental determination of the rate constants for reactions b and c.
2. Inclusion of the reactions resulting in the formation of NH_3.
3. Expansion of the model to include lasing energy produced and percentage of energy lost due to the experimental setup.

B. EXPERIMENTAL

1. A gain experiment to determine the existence of laser action.

2. The use of a partial transmitting mirror as part of the laser cavity to reduce the amount of energy removed from the cavity on each pass.

3. Procurement of a Trigger Pulse Generator to reduce the electrical noise picked up by the recording equipment.

4. Inclusion of a storage system for HN_3 in the experimental setup. This would reduce exposure to the toxic chemicals used to generate HN_3 to allow more experiments per generation.

5. Extension of the laser cavity to increase the laser gain on each pass through the cavity.

6. The use of a rapid frequency scanner to determine the wavelength of laser action.

7. Operation of the laser tube as a pure $CO_2 + N_2$ laser by high voltage excitation would also provide the necessary alignment information.

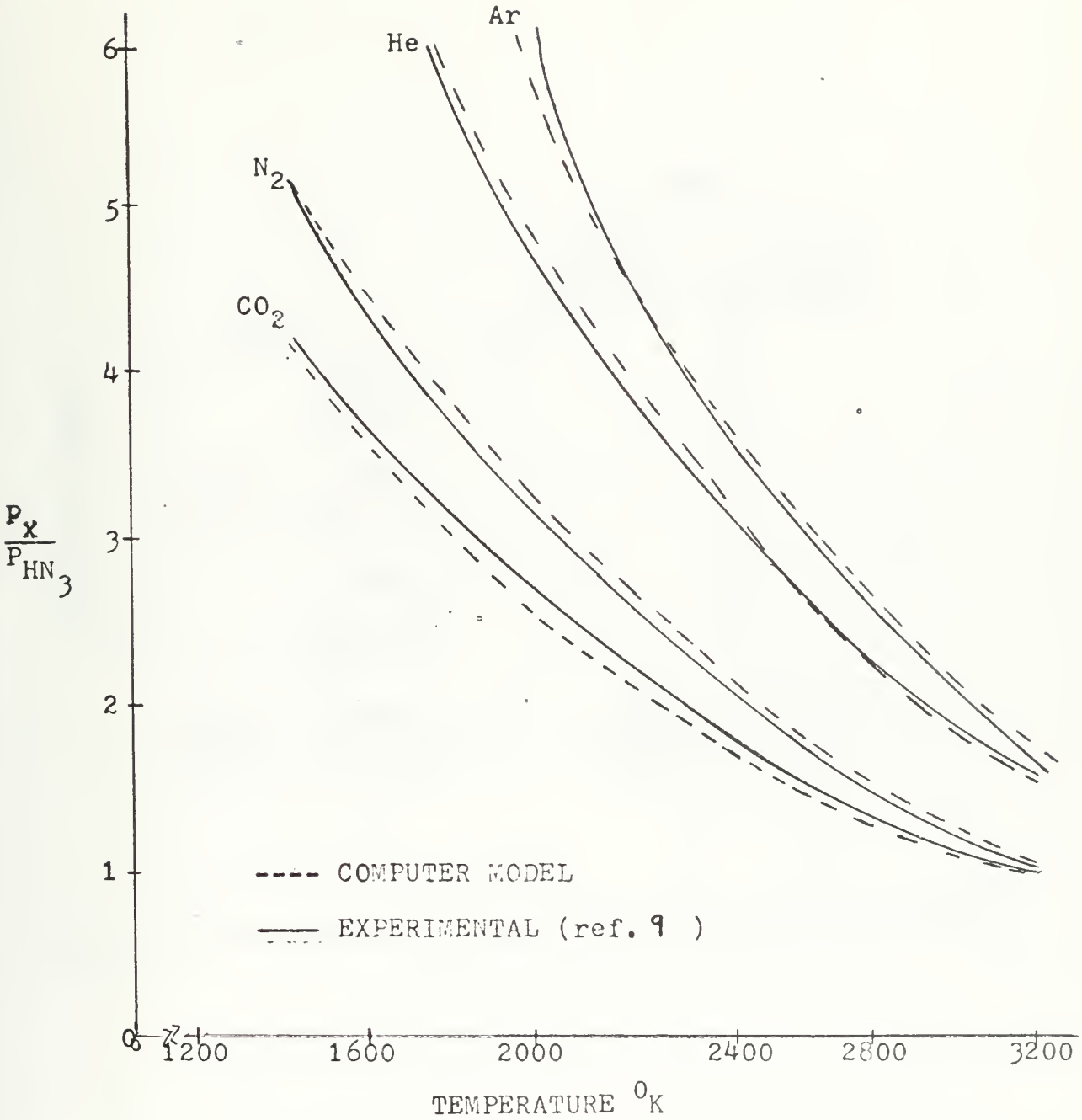

COMPARSION OF THEORTICAL AND EXPERIMENTAL ADIABATIC TEMPERATURE FOR VARIOUS DILUTION OF HN_3.

Figure 1 .

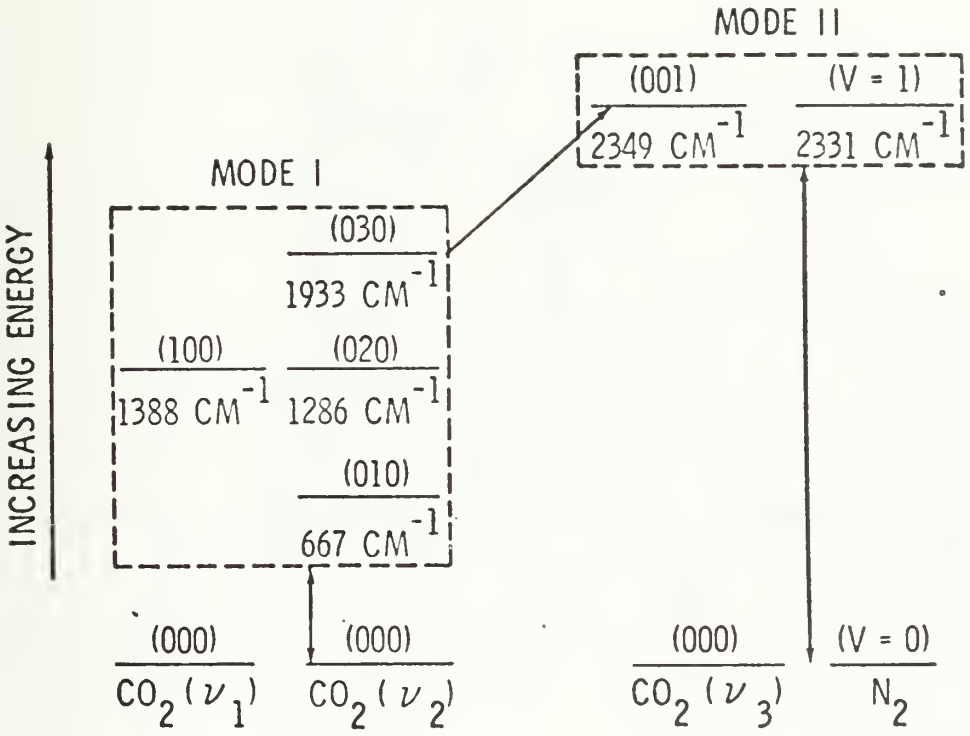

SCHEMATIC OF THE GROUPING OF ENERGY LEVELS FOR THE VIBRATIONAL MODEL

Figure 2.

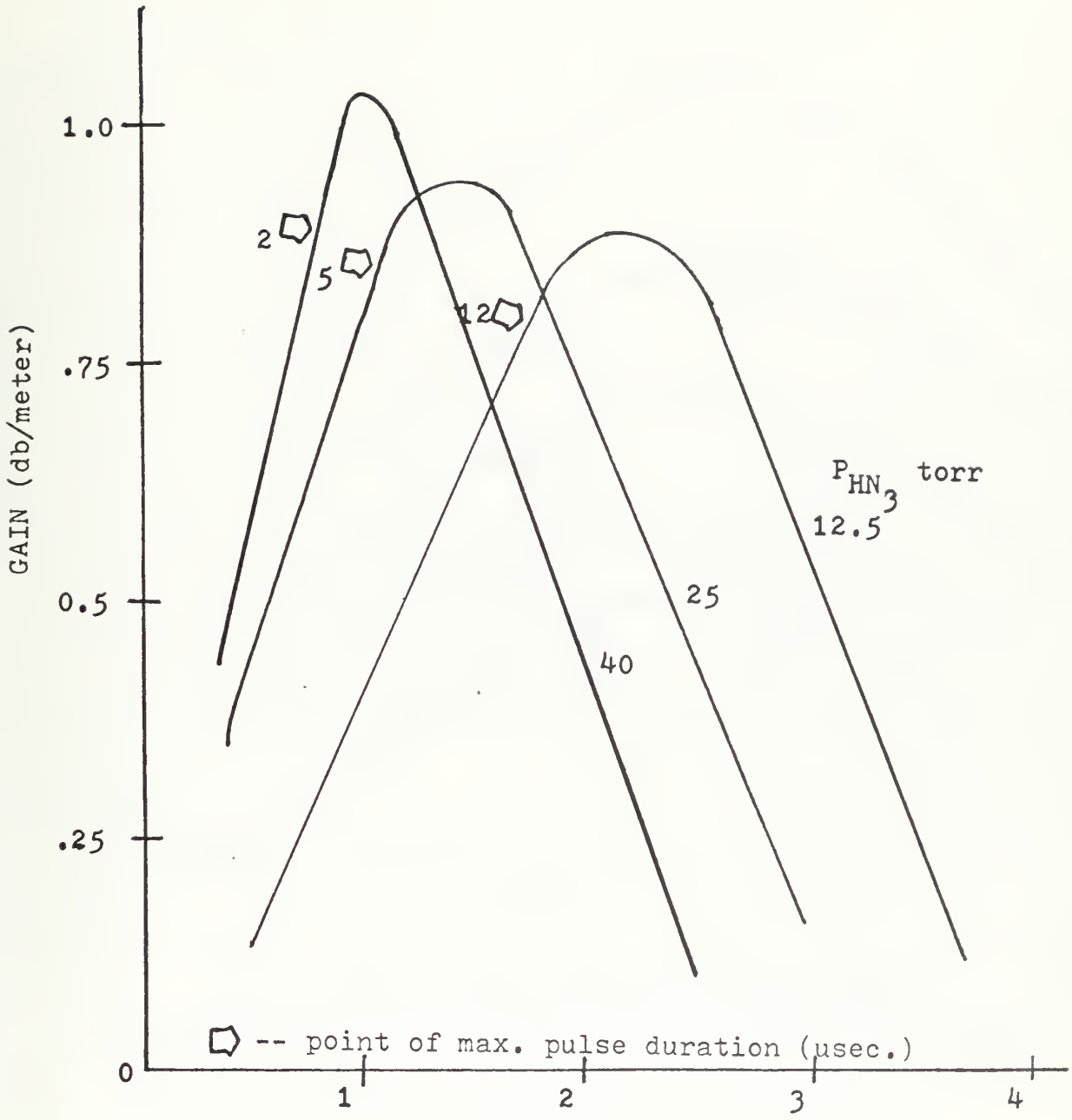

Figure 3. Resulting Gain from dilution of HN_3 with CO_2.

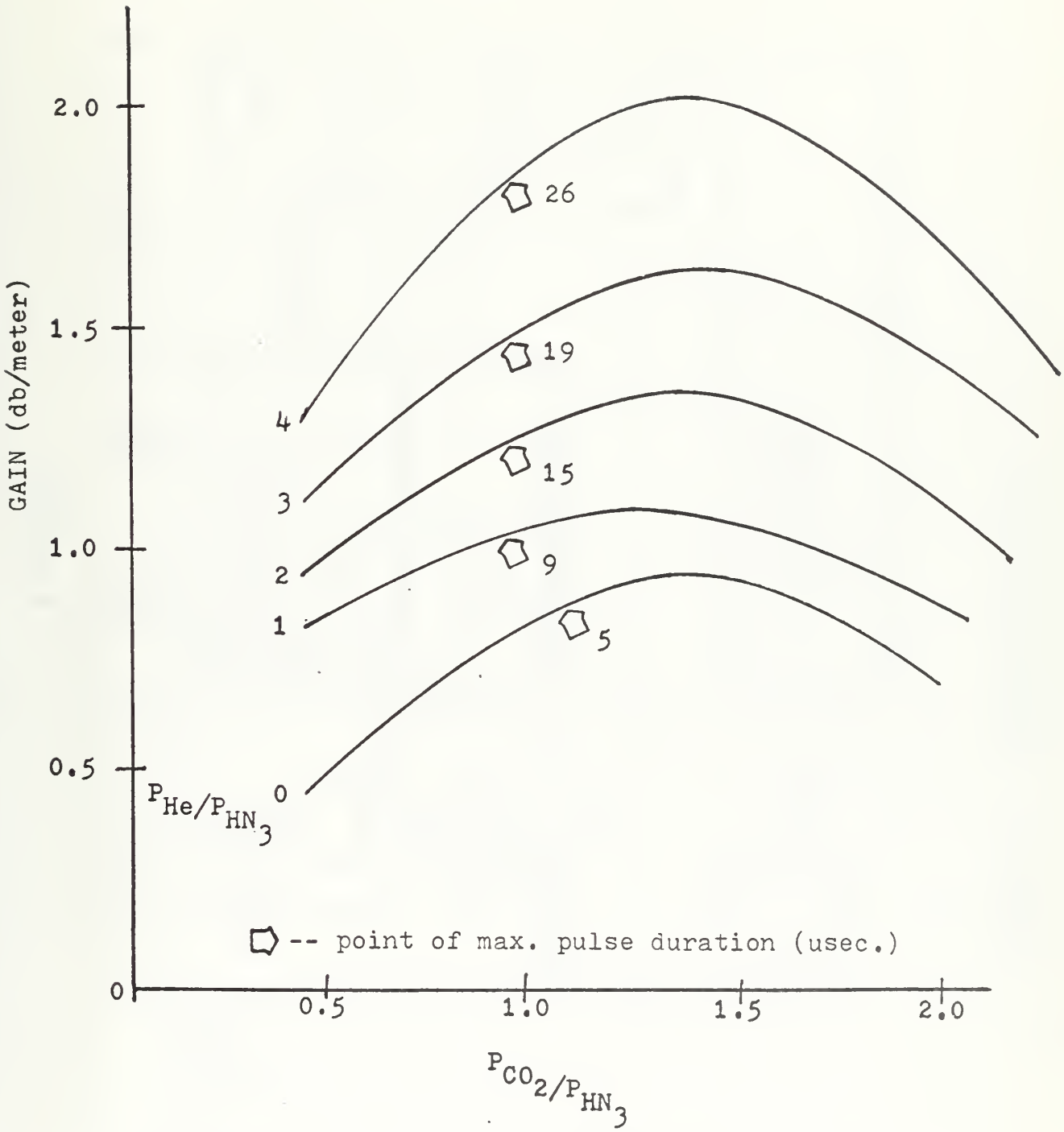

Figure 4. Increase in Gain resulting from the addition of He to an HN_3 + CO_2 mixture.

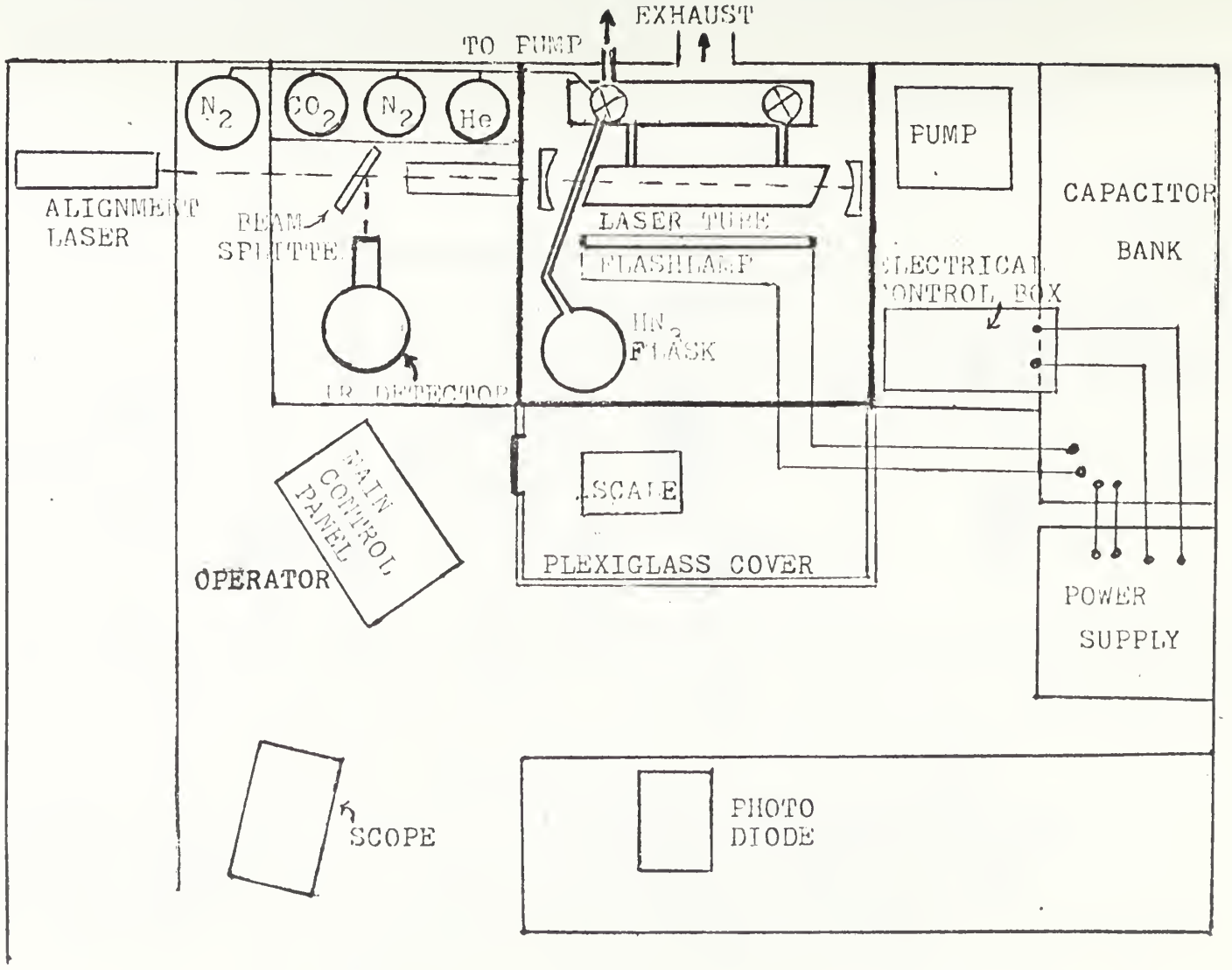

Figure 5 . Experimental Setup

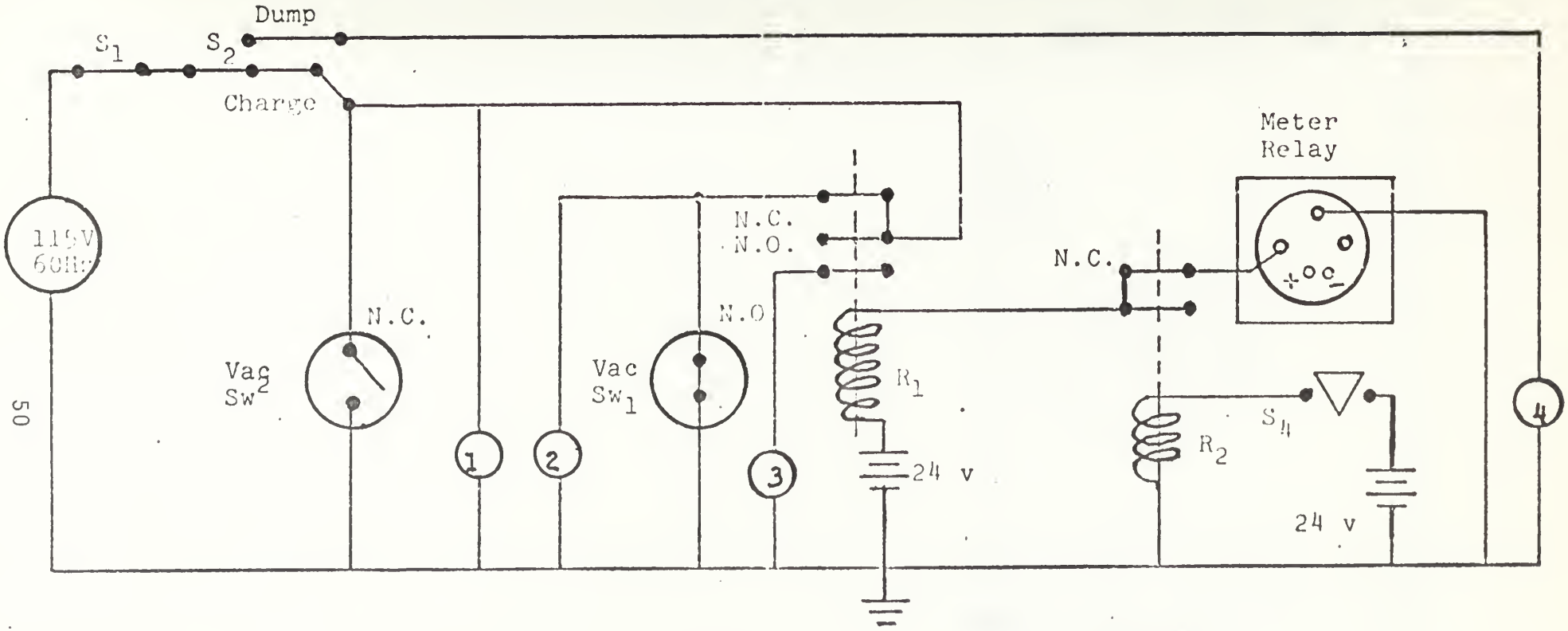

S_1: On-Off switch
S_2: Door safety interlock
S_3: Charge-Dump switch
S_4: "Fire" push button
R_1, R_2: 24 v DC Relay

1: Charge warning flasher
2: "Charging" indicator light
3: "Ready" indicator light
4: "Dumped" indicator light
N.O.: Normally open
N.C.: Normally closed

Figure 6. Schematic of the Electrical Control Box

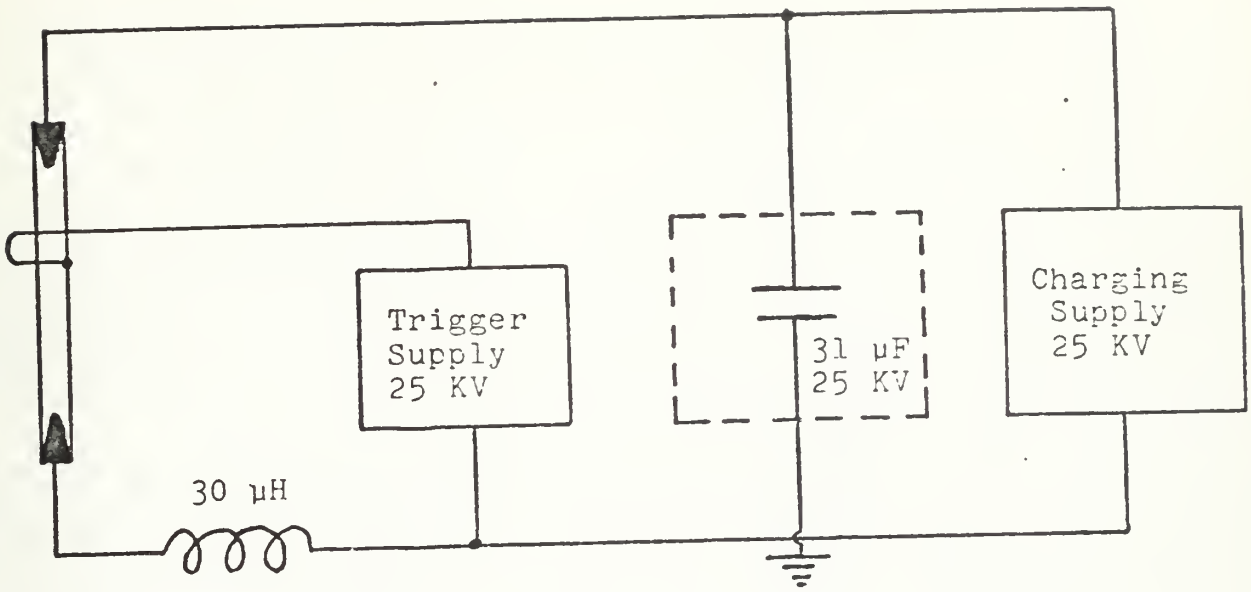

Figure 7 . Flashlamp Discharge Circuit

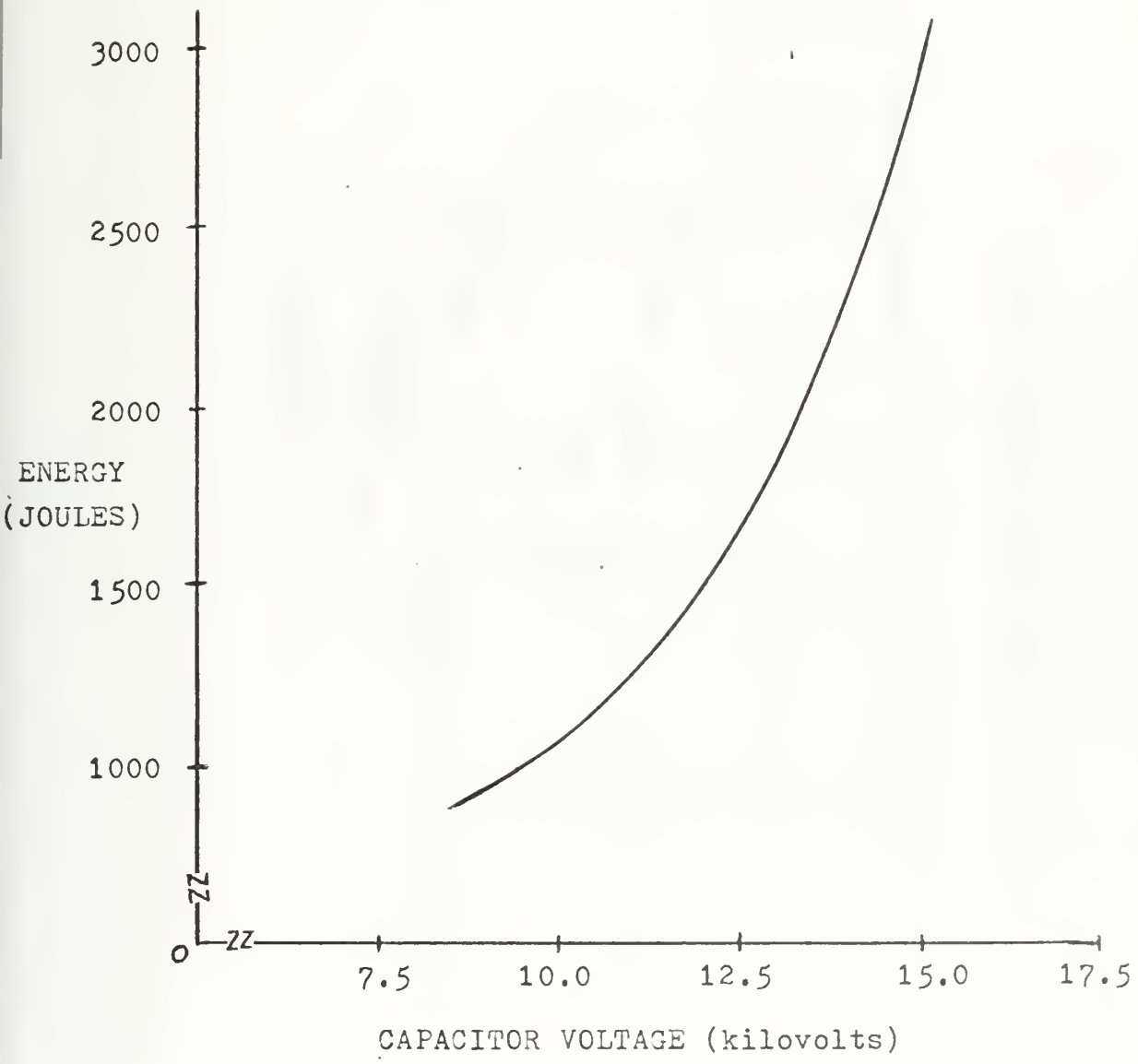

Figure 8 . Flash Energy vs. Capacitor Voltage

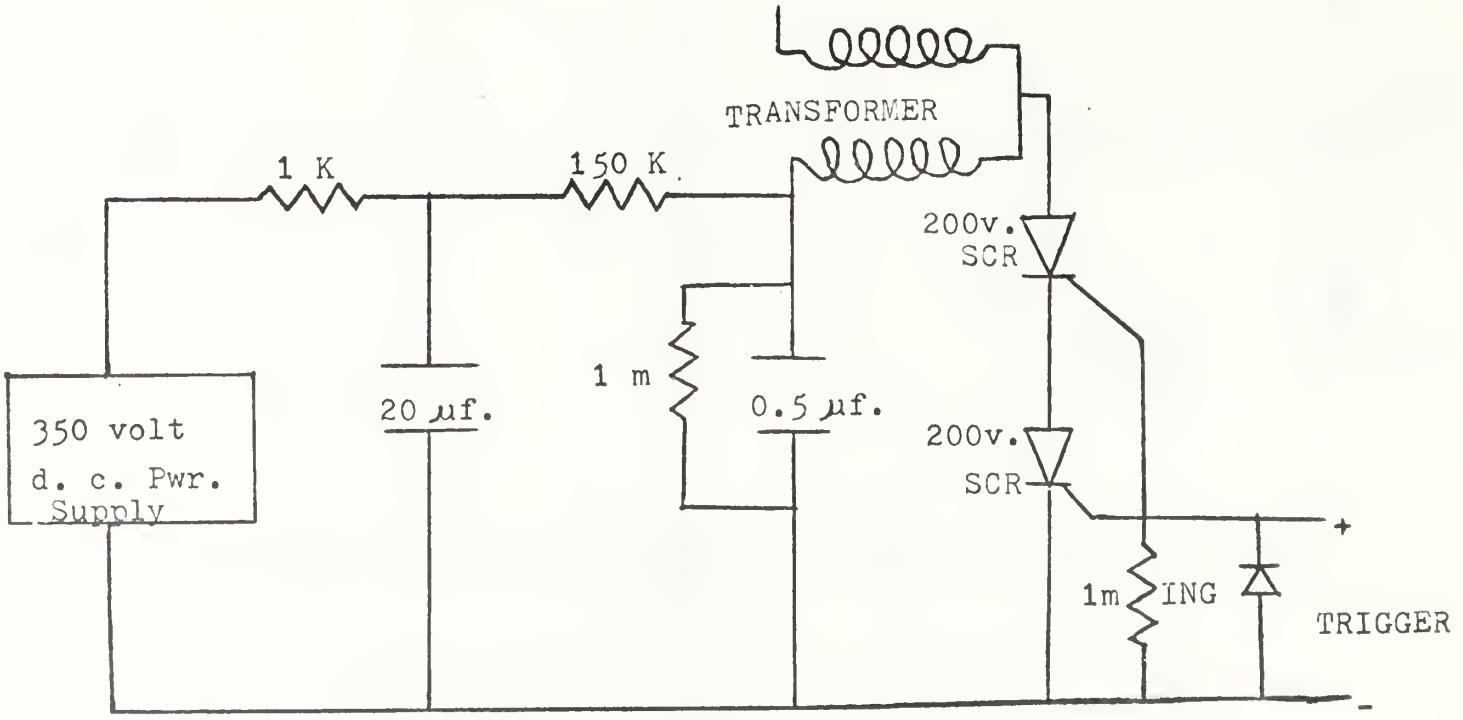

Figure 9 . Flash Lamp Trigger Circuit

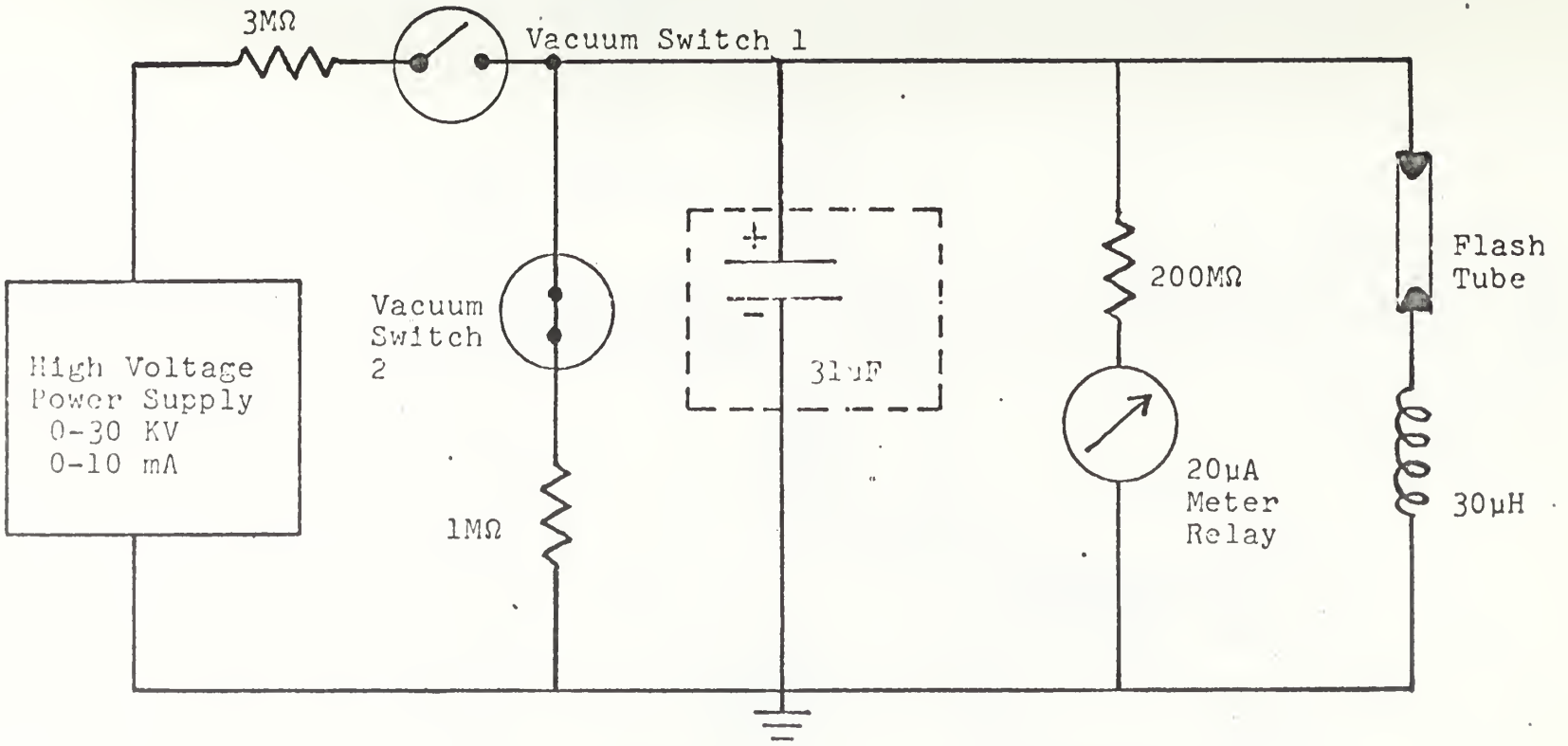

Figure 10. Block Diagram of Charging System.
Vacuum switches 1 and 2 are shown in normal (de-energized) position.

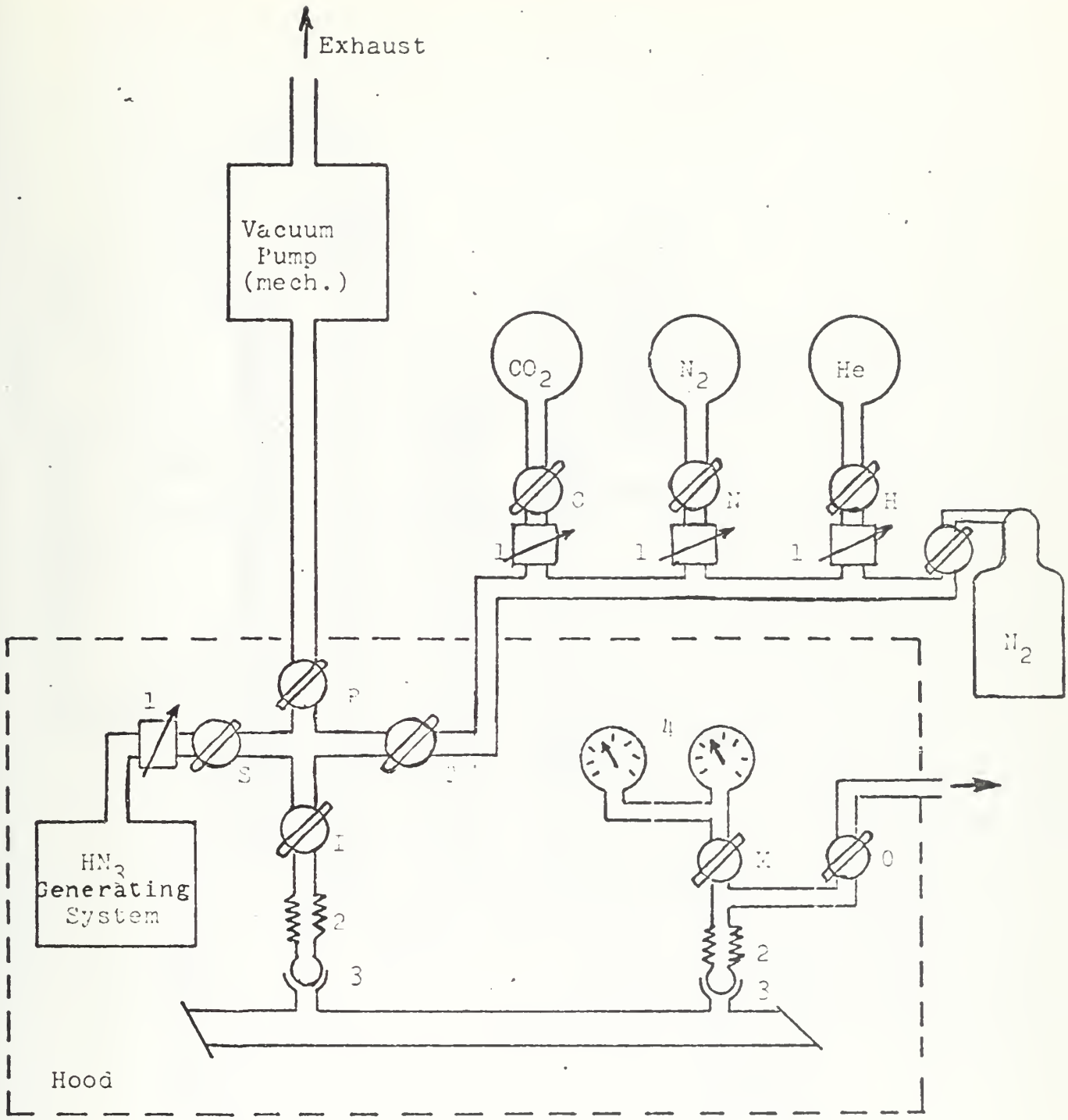

1. Needle valve and bypass
2. Stainless steel bellows
3. Balljoints
4. Bourdon tube and thermocouple gauge

Figure 11. Vacuum System

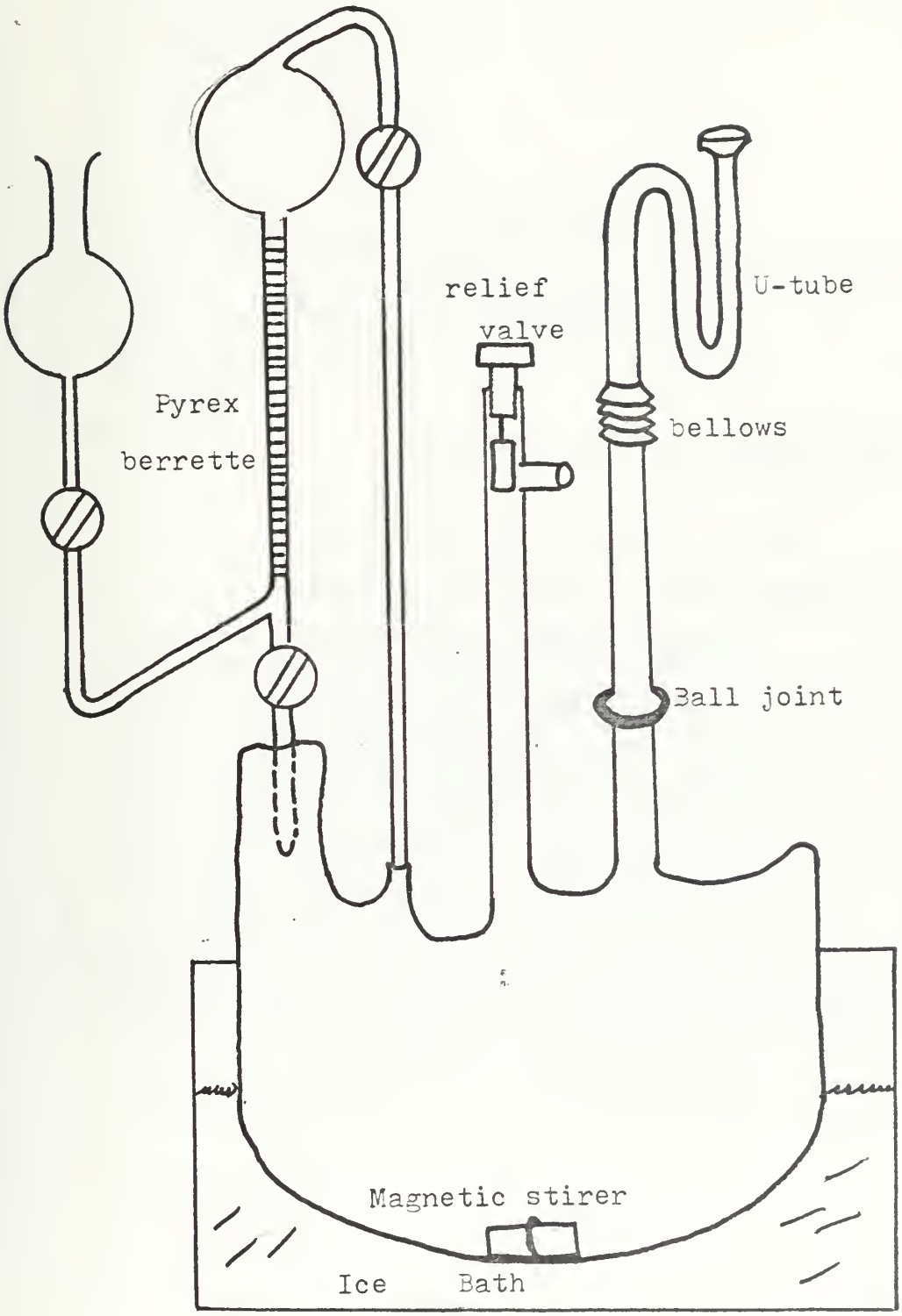

Figure 12. HN_3 Gas Generator

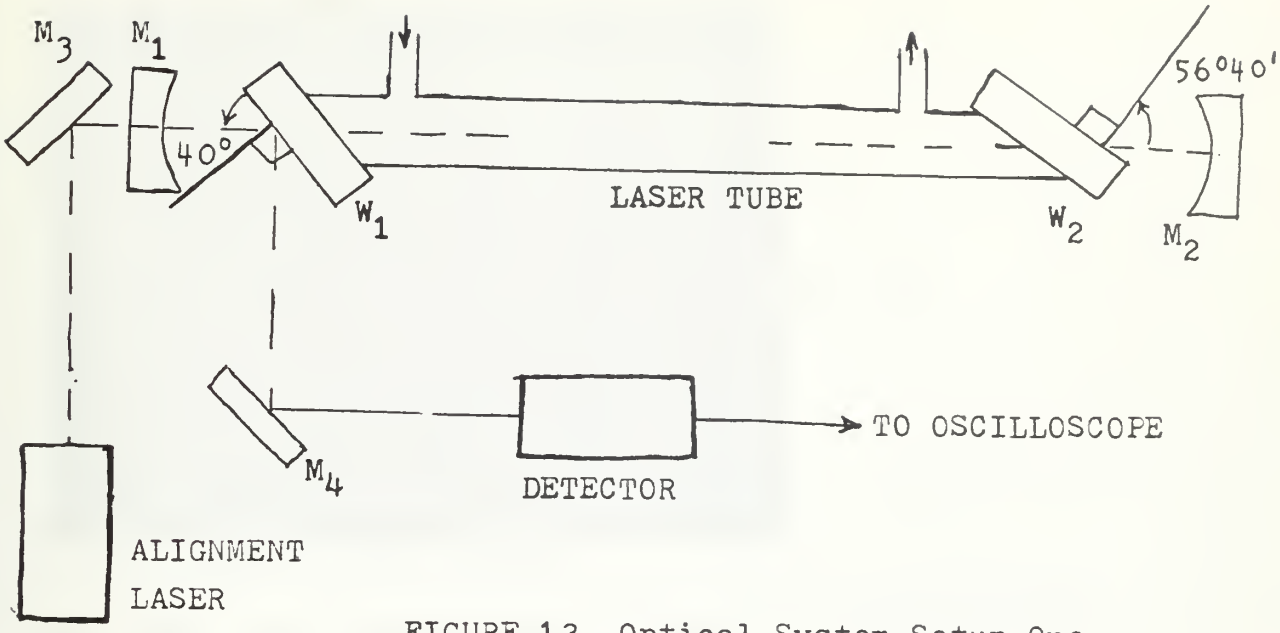

FIGURE 13. Optical System Setup One

M_1, M_2: Concave cavity mirrors

M_3, M_4: Plane front coated mirrors

W_1, W_2: NaCl laser windows

Y_1: NaCl beam splitter

Z_1: 2 mm. hole

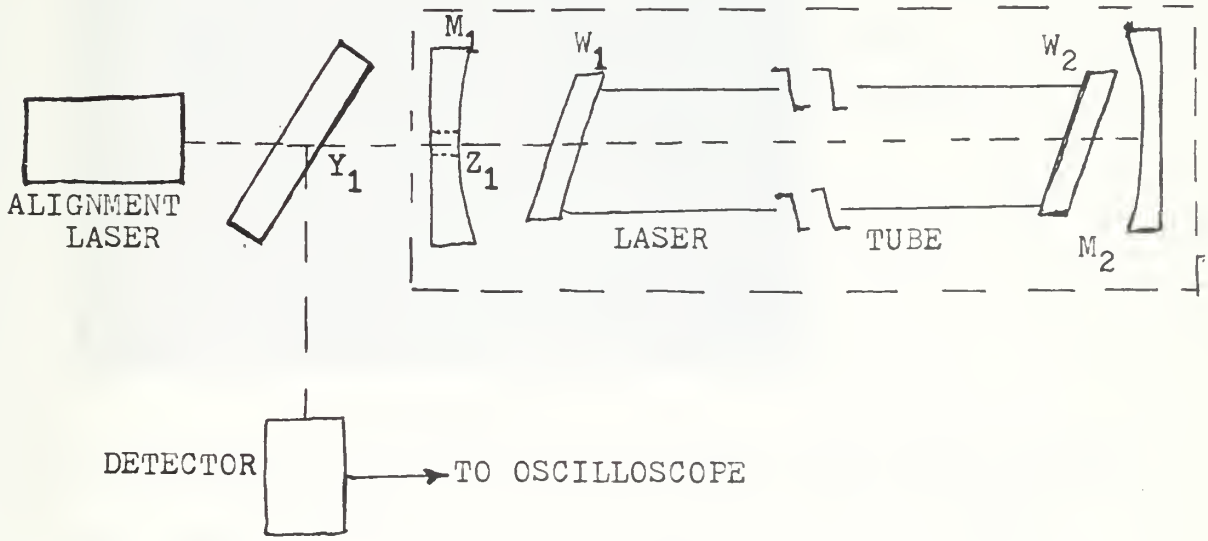

FIGURE 14. Optical System Setup Two

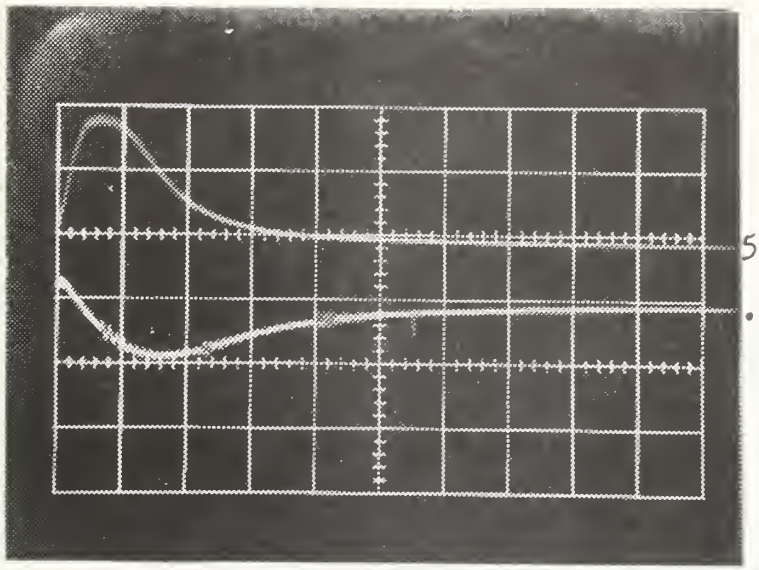

Figure 15. Oscilloscope trace of output from Photo Diode (upper) and IR Detector with 10.2 filter (lower).

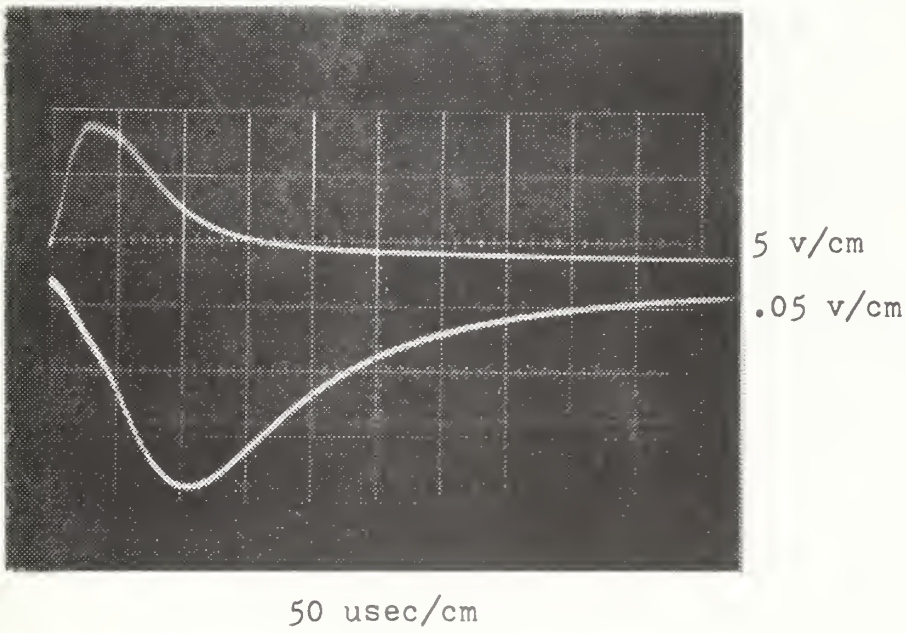

Figure 16. Oscilloscope trace of output from Photo Diode (upper) and IR Detector with Irtran II filter (lower).

HN_3 torr	NaN_3 grams	H_3PO_4 grams
10	0.0382	0.0576
20	0.0764	0.1153
30	0.1132	0.1729
40	0.1520	0.2305
50	0.1900	0.2880

TABLE I. Amounts of NaN_3 and H_3PO_4 necessary to generate a desired pressure of HN_3 in a one liter system.

APPENDIX A: REACTIONS AND RATE CONSTANTS USED IN THE COMPUTER MODEL

All rate constants are in the units of: $part.^{-1} cc.sec^{-1}$

$HN_3 \dashrightarrow \dot{N}H + N_2^*$

$KHV = 2.89 \times 10^{15} t^3 - 6.4 \times 10^{11} t^2 + 3.42 \times 10^{7} t$

$N_2^* + HN_3 \rightarrow \dot{N}H + N_2' + N_2$

$K2 = 7.64 \times 10^{-9} e^{-6400/RT}$

$\dot{N}H + HN_3 \rightarrow H_2 + 2N_2^*$

$K3 = 8.7 \times 10^{-7} e^{-8210/RT}$

$NH + NH \rightarrow H_2 + N_2'$

$K4 = 3.6 \times 10^{-12} T^{0.55} e^{-1900/RT}$ (Ref. 33)

$N_2^\# + M \rightarrow N_2 + M$

This equation as stated before is only a representation of the reactions that must be considered in the computer model. The following equations are those actually required for each diluent considered.

$N_2' + H_2 \rightarrow N_2 + H_2$

$K = e^{-8.76T^{-1/3} - 2.23}$

N_2 (MODE II) + $CO_2 \longleftrightarrow N_2 + CO_2$ (MODE II)

$K = e^{-0.0472T^{1/2} - 27.36}$ for $T \leq 1000°K$

$K = e^{0.153T^{1/2} - 33.83}$ for $T \geq 1000°K$ (Ref. 29)

N_2(MODE II) + He --> N_2 + He

$$K = 1.36\times10^{-16} T\ 10^{-(60.7T^{-1/3}-4.168)}$$ (Ref. 24)

CO_2(MODE I) + CO_2 --> CO_2 + CO_2

$$K = 1.36\times10^{-16} T\ 10^{-(17.8T^{-1/3}-1.808)}$$ (Ref. 24)

CO_2(MODE I) + H_2 --> CO_2 + H_2

$$K = 4.0\times10^{-12}$$ (Ref. 29)

CO_2(MODE I) + N_2 --> CO_2 + N_2

$$K = 3.4\times10^{-17} T\ 10^{-(17.8T^{-1/3}-1.808)}$$ (Ref. 24)

CO_2(MODE II) + He --> CO_2 + He

$$K = 3^{-46.23T^{-1/3}-23.01}$$ (Ref. 29)

CO_2(MODE II) + CO_2 --> CO_2(MODE I) + CO_2

$$K = 6.55\times10^{-11} T^{-0.1293}$$ (Ref. 29)

CO_2(MODE II) + H_2 --> CO_2 + H_2

$$K = 5.0\times10^{-14}$$ (Ref. 29)

CO_2(MODE II) + He --> CO_2(MODE I) + He

$$K = 5.895\times10^{-11} T^{-0.1293}$$ (Ref. 24

CO_2 + CO_2 --> CO_2(MODE I) + CO_2

$$K = 1.36\times10^{-17.808-17.8T^{-1/3}}$$ (Ref. 24)

$$CO_2(\text{MODE I}) + CO_2 \dashrightarrow CO_2(\text{MODE II}) + CO_2$$

$$K = 6.55\times10^{-11}T^{-0.1293}e^{-1431.5/T_{vib}} \qquad \text{(Ref. 24)}$$

```
C
C          APPENDIX B: HN3 + CO2 LASER PROGRAM
C
C
C
C         THIS PROGRAM CALCULATES THE POPULATION INVERSION
C
C
C         AND LASER GAIN PRODUCED WITHIN CO2
C
C
      IMPLICIT REAL*8 (A-H,K,O-Z)
      REAL*4 XGPH,YGPH,T,G0,G2,G9
      DIMENSION F(17),Y(17),XGPH( 200),YGPH( 200),T(200)
     1,G2(200),G9(200),R(10,10)
C
C         MOLAR GAS CONSTANT
      RO=62361.0
C         STEP SIZE
      H=1.0D-08
C         NO. OF EQUATIONS TO BE INTEGRATED
      N=17
C         INITIAL TIME
      X=0.0D0
C         THETA V OF THE FIRST VIBRATIONAL LEVEL OF N2
      HNV1=-3354.301991
C         LOSCHMIDT'S NUMBER
      AL=2.6874D19
C         AVOGADRO'S NUMBER
      AN=6.0254D23
C         INITIAL VALUES FOR CONTROL OF OUTPUT AND INTEGRATION
      M=1
      MM=1
      NN=1
      I=1
      JJ=1
      NT=0
      U=0.0
      GO=0.0D0
C
C
C         INITIAL CONSENTRATIONS OF REACTANTS
C
C         Y(1)--HN3
C
C         Y(2)--HN
C
C         Y(3)--H2
```

```
C                                                                       00000490
CC          Y(4)--N2 (GND. LEVEL)                                       00000500
CC                                                                      00000510
CC          Y(5)...Y(13)---N2 (V=1...9,LEVEL)                           00000520
CC                                                                      00000530
CC          Y(14)= CO2 GND STATE                                        00000540
CC                                                                      00000550
CC          Y(15)= CO2 MODE II (V=1 & V=2 LEVELS)                       00000560
CC                                                                      00000570
CC          Y(16)= CO2 MODE I (V=3 LEVEL)                               00000580
CC                                                                      00000590
CC          Y(17)--TEMP.                                                00000600
CC                                                                      00000610
                                                                        00000620
      DO 1 M=1,N                                                        00000630
      Y(M)=0.0D0                                                        00000640
    1 CONTINUE                                                          00000650
      Y(17)=300.0                                                       00000660
      Y(1)=(25.00/(RO*Y(17)))*AN                                        00000670
      Y(14)=(  12.50/(RO*Y(17)))*AN                                     00000680
      HE=(100.0/(RO*Y(17)))*AN                                          00000690
C           CO2= TOTAL CONC. OF CARBON DIOXIDE                          00000700
      CO2=Y(14)                                                         00000710
C           VIBRATIONAL TEMP. OF N2                                     00000720
C           VIBRATIONAL TEM. OF N2 (V=0,1)                              00000730
      TV=Y(17)                                                          00000740
C           OUTPUT OF INITIAL VALUES                                    00000750
      WRITE (6,101)                                                     00000760
      WRITE(6,102)U,Y(17),Y(1),Y(2),Y(4),Y(5),Y(14),Y(15),Y(16),GO      00000770
C           INITIALIZE THE MATRIX FOR THE TRANSTION PROBILITIES         00000780
C           OF PURE N2                                                  00000790
      DO 6 L=1,10                                                       00000800
      DO 6 LL=1,10                                                      00000810
    6 R(L,LL)=0.0D0                                                     00000820
C                                                                       00000830
C           OUTSIDE DO LOOP FOR INTEGRATION OF THE RATE EQ.'S           00000840
   22 FT=0.0                                                            00000850
C                                                                       00000860
CC          SPECIFIC HEAT AT CONSTANT VOLUME                            00000870
CC                                                                      00000880
C           FOR H2                                                      00000890
      CVH=5.76+5.78D-04*1.8*Y(17)+(20.0/(1.8*Y(17))**0.5D0)-1.987       00000900
C           FOR CO2                                                     00000910
      CVC=16.1-(6530.0/(1.8*Y(17)))+(1.41D06/(1.8*Y(17))**2)-1.987      00000920
C           FOR N2                                                      00000930
      CVN=9.47-(3470.0/(1.8*Y(17)))+(1.16D06/(1.8*Y(17))**2)-1.987      00000940
      IF(Y(17).GT.2500.0) CVH=CVN                                       00000950
C           CALCULATE THE TOTAL CONC. OF N2                             00000960
```

```
      DO 2 J=4,13                                                       00000970
    2 FT=FT+Y(J)                                                        00000980
C           RELAXATION RATES TO BE USED IN CAL. OF                      00000990
C           RATE CONSTANTS                                              00001000
      TPA=(1.3D05*(1.0D0/Y(17)**(1.0D0/3.0D0))**4.9)                    00001010
      TC2=(10.0D0**(17.8*(1.0D0/Y(17)**(1.0D0/3.0D0))-1.808))           00001020
C                                                                       00001030
C           REACTIONS FOR CAL. OF LASER GAIN WITH                       00001040
C           RATE CONSTANTS FOR EACH REACTION LISTED BELOW IT            00001050
C                                                                       00001060
C           HN3 -HV-> HN +N2                                            00001070
      KHV=0.0D0                                                         00001080
      IF(X.GT.100.0D-06) GO TO 4                                        00001090
      KHV=2.84D15*X**3-6.40D11*X**2+3.42D07*X                           00001100
C                                                                       00001110
C           N2* +HN3 --> HN + N2 + N2(V=1)                              00001120
    4 K1=7.64D-09*DEXP(-6400.0/(1.987*Y(17)))                           00001130
C                                                                       00001140
C           HN +HN3 --> H2 + 2N2*                                       00001150
      K2=8.70D-07*DEXP(-8210.0/(1.987*Y(17)))                           00001160
C                                                                       00001170
C           HN + HN --> H2 + N2                                         00001180
      K3=3.6D-12*Y(17)**0.55*DEXP(-1900.0/(1.987*Y(17)))                00001190
C                                                                       00001200
C           N2(V=1) + H2 ---> N2 + H2                                   00001210
      K4=DEXP(-8.760389087D01*(Y(17)**(-1.0D0/3.0D0))-2.231265144D01)   00001220
C                                                                       00001230
C           N2(V=1) + CO2 <---> N2 + CO2 (MODE II)                      00001240
      K5=DEXP(-4.719388646D-02*Y(17)**0.5D0-27.35760188)                00001250
      IF(Y(17).GT.1000.0D0) K5=DEXP(1.526181091D-01*Y(17)**0.5D0        00001260
     1-33.83415823)                                                     00001270
C                                                                       00001280
C           CO2(NII) + HE ---> CO2(NI) + HE                             00001290
      K6=Y(17)*1.0D06/(TPA*AL*273.0)                                    00001300
C                                                                       00001310
C           CO2(NII) + H2 ---> CO2 + H2                                 00001320
      K7=5.0D-14                                                        00001330
C                                                                       00001340
C           CO2(NI) + H2 ---> CO2 + H2                                  00001350
      K8=4.0D-12                                                        00001360
C                                                                       00001370
C           CO2(NI) + CO2 ---> CO2 + CO2                                00001380
      K9=Y(17)*1.0D06/(TC2*AL*273.0)                                    00001390
C                                                                       00001400
C           CO2(NI) + N2 ---> CO2 + N2                                  00001410
      K10=0.25D0*K9                                                     00001420
C                                                                       00001430
C           CO2(NII) + CO2 ---> CO2(NI) + CO2                           00001440
```

```
      K11=K6/0.27D0                                                          00001450
C                                                                            00001460
C           CO2(NI) + HE ---> CO2 + HE                                       00001470
      K12=DEXP(-46.22873949D0*Y(17)**(-1.0D0/3.0D0)-23.00814718)             00001480
C                                                                            00001490
C           N2(V=1) + HE ---> N2 + HE                                        00001500
      K13=Y(17)*1.0D06/(10.0D0**((60.7*Y(17)**(-1.0D0/3.0D0))-4.168)         00001510
     1*AL*273.0)                                                             00001520
C                                                                            00001530
C           CO2 + CO2 ---> CO2 + CO2(NI)                                     00001540
      K14=K9*DEXP(- 960.0/Y(17))                                             00001550
C                                                                            00001560
C           CO2 + CO2(NI) ---> CO2 + CO2(NII)                                00001570
      K15=K11*DEXP(-1431.5/TV)                                               00001580
C                                                                            00001590
CC          TRANSITIONS PROBABLITIES FOR N2 VIB LEVELS                       00001600
C                                                                            00001610
      R(2,1)=(AL*273.0/Y(17))*DEXP(-290.457*Y(17)**(-1.0/3.0)-12.5062)       00001620
      IF(Y(17).GT.1953.0) R(2,1)=(AL*273.0/Y(17))*DEXP(-56.6866*             00001630
     1Y(17)**(-1.0/3.0)-31.20782)                                            00001640
      IF(Y(5).LT.10.0) GO TO11                                               00001650
C           CAL. OF THE VIBRATIONAL TEMP. OF N2                              00001660
      TV=HNV1/DLOG(Y(5)/Y(4))                                                00001670
   11 IF(TV.LT.Y(17)) TV=Y(17)                                               00001680
      R(1,2)=R(2,1)*DEXP(HNV1/TV)                                            00001690
      DO 5 LL=2,9                                                            00001700
      R(LL+1,LL)=DFLOAT(LL)*9.6544D03*DSQRT(Y(17))                           00001710
      R(LL,LL+1)=R(LL+1,LL)*DEXP(HNV1/TV)                                    00001720
    5 CONTINUE                                                               00001730
C                                                                            00001740
CC          RATE EQ'S. FOR Y(1)...Y(17)                                      00001750
C                                                                            00001760
      F(1)=-K1*Y(1)*Y(13)-K2*Y(2)*Y(1)-KHV*Y(1)                              00001770
      F(2)=K1*Y(1)*Y(13)-K2*Y(2)*Y(1)                                        00001780
     1-K3*2.0*Y(2)**2+KHV*Y(1)                                               00001790
      F(3)=K2*Y(2)*Y(1)+K3*Y(2)**2                                           00001800
      F(13)=-K1*Y(13)*Y(1)+K2*2.0*Y(2)*Y(1)+KHV*Y(1)-R(10,9)*Y(13)           00001810
     1+R(9,10)*Y(12)                                                         00001820
      F(4)=K1*Y(13)*Y(1)+K4*Y(5)*Y(3)                                        00001830
     1+R(2,1)*Y(5)-R(1,2)*Y(4)-K5*Y(16)*Y(4)+K5*Y(14)*Y(5)                   00001840
     2+K13*Y(5)*HE                                                           00001850
      F(5)=R(1,2)*Y(4)+R(3,2)*Y(6)-R(2,3)*Y(5)-R(2,1)*Y(5)+K1*Y(13)*Y(1)     00001860
     1-K4*Y(5)*Y(3)-K5*Y(14)*Y(5)+K5*Y(16)*Y(4)-K13*Y(5)*HE+K3*Y(2)**2       00001870
      DO 3 L=3,9                                                             00001880
      F(L+3)=R(L-1,L)*Y(L+2)+R(L+1,L)*Y(L+4)-R(L,L-1)*Y(L+3)                 00001890
     1-R(L,L+1)*Y(L+3)                                                       00001900
    3 CONTINUE                                                               00001910
      F(14)=K5*Y(16)*Y(4)+K8*Y(15)*Y(3)+K9*Y(15)*Y(14)-K14*Y(14)**2           00001920
```

```
     1+K10*Y(15)*Y(4)-K5*Y(14)*Y(5)+K12*Y(15)*HE                                00001930
      F(15)=K6*Y(16)*Y(4)+K7*Y(16)*Y(3)+K11*Y(16)*Y(14)-K8*Y(15)*Y(3)           00001940
     1-K9*Y(15)*Y(14)-K10*Y(15)*Y(4)+K6*Y(16)*HE-K12*Y(15)*HE                   00001950
     2+K14*Y(14)**2-K15*Y(15)*Y(14)                                            00001960
      F(16)=K5*Y(14)*Y(5)-K6*Y(16)*Y(4)-K7*Y(16)*Y(3)-K11*Y(16)*Y(14)          00001970
     1-K5*Y(16)*Y(4)-K6*Y(16)*HE+K15*Y(15)*Y(14)                               00001980
      F(17)=(79.0D03*K2*Y(1)*Y(2)+17.0D03*K1*Y(13)*Y(1)+115.0D03*K3*Y(2        00001990
     1)**2+13.0D03*KHV*Y(1))/(CVH*Y(3)+CVC*CO2                                 00002000
     2+CVN*FT+(13.0)*Y(1)+CVN*Y(2)+2.98*HE)                                    00002010
C                                                                              00002020
CC          INTEGRATING SUBROUTINE                                             00002030
C                                                                              00002040
      S=RKLDEQ(N,Y,F,X,H,NT)                                                   00002050
      DO 7 ML=1,16                                                             00002060
    7 IF(Y(ML).LT.1.0D0   ) Y(ML)=0.0D0                                        00002070
      IF(Y(1).LT.1.0D09) Y(1)=0.0D0                                            00002080
      IF(S-1.0)22,22,40                                                        00002090
C                                                                              00002100
CC          ADJUST STEP SIZE AND AMOUNT OF PRINT OUT                           00002110
C                                                                              00002120
   40 IF(I-MM)12,13,12                                                         00002130
   13 U=X*1.0D06                                                               00002140
      WRITE(6,102)U,Y(17),Y(1),Y(2),Y(4),Y(5),Y(14),Y(15),Y(16),GO             00002150
      NN=NN+1                                                                  00002160
      MM=MM+50                                                                 00002170
      IF(NN.EQ.75) WRITE(6,101)                                                00002180
      IF(NN.EQ.75) NN=1                                                        00002190
   12 IF(Y(17).GT.500.0) H=1.0D-09                                             00002200
      IF(Y(2).GT.1.0D15) H=1.0D-10                                             00002210
      IF(Y(1).LT.1.0D08) H=1.0D-08                                             00002220
      IF(X.LT.5.0D-06) GO TO 15                                                00002230
      GO=5.893826821D-12*((Y(16)-Y(15))/Y(17)**1.5D0)*                         00002240
     1DEXP(-987.32/Y(17))                                                      00002250
      IF(JJ.GT.1) GO TO 16                                                     00002260
      IF(GO.LT.1.0D-05) GO TO 15                                               00002270
   16 IF(I-M) 14,17,14                                                         00002280
C                                                                              00002290
CC          QUANTIES TO BE PLOTTED                                             00002300
C                                                                              00002310
   17 M=M+28                                                                   00002320
      XGPH(JJ)=X*1.0D06                                                        00002330
      YGPH(JJ)=(Y(16)-Y(15))/(Y(16)+Y(14)+Y(15))                               00002340
      G2(JJ)=5.893826821D-12*((Y(16)-Y(15))/Y(17)**1.5D0)*                     00002350
     1DEXP(-987.32/Y(17))                                                      00002360
      T(JJ)=TV                                                                 00002370
      JJ=JJ+1                                                                  00002380
      GO TO 14                                                                 00002390
   15 M=I+1                                                                    00002400
```

```
   14 I=I+1                                                              00002410
      IF(X.GT.3.0D-03) GO TO 99                                          00002420
      IF(JJ.LT.201) GO TO 22                                             00002430
C                                                                        00002440
CC          CALL PLOT SUBROUTINE                                         00002450
C                                                                        00002460
      WRITE(6,103)                                                       00002470
      CALL PLOTP(XGPH,YGPH,200,0)                                        00002480
      WRITE(6,103)                                                       00002490
      CALL PLOTP(XGPH,G2,200,0)                                          00002500
      WRITE(6,103)                                                       00002510
      CALL PLOTP(XGPH,T   ,200,0)                                        00002520
  101 FORMAT('1',6X,'TIME USEC',3X,'TEMP.  K',7X,'HN3',10X,              00002530
     1'HN',10X,'N2',9X,'N2 (V=1)',8X,'CO2',6X,'CC2 MODE I',              00002540
     23X,'CO2 MODE II',6X,'GAIN',//)                                     00002550
  102 FORMAT (' ',2F13.2,7D13.2,1F13.2)                                  00002560
  103 FORMAT('1',///)                                                    00002570
   99 STOP                                                               00002580
      END                                                                00002590
```

```
C
C
C
C     RKLDEQ INTEGRATING SUBROUTINE
C
C
C
C
C
C
C
C
      DOUBLE PRECISION FUNCTION RKLDEQ (N,Y,F,X,H,NT)
      REAL*8 Y,F,X,H,Q,H1,H2,H3,H6
      DIMENSION Y( N), F( N) ,Q(25)
      NT = NT +1
      GO TO (1,2,3,4),NT
    1 H1 = H
      H2 = H1 * .5D0
      H3=H1*2.0D0
      H6 = H1/6.D0
      DO 11 J =1,N
   11 Q(J) = 0.D0
      A = .5D0
      X = X + H2
      GO TO 5
    2 A = .292893218813452
      GO TO 5
    3 A = 1.707106781186547
      X = X + H2
      GO TO 5
    4 DO 41 I = 1,N
   41 Y(I) = Y(I) + H6 * F(I) -Q(I)/3.D0
      NT = 0
      RKLDEQ =2.
      GO TO 6
    5 DO 51 L = 1,N
      Y(L) = Y(L) + A *(H * F(L) -Q(L))
   51 Q(L) = H3 * A *F(L) +(1.D0-3.D0*A) *Q(L)
      RKLDEQ =1.
    6 RETURN
      END
```

COMPUTER PROGRAM OUTPUT

TIME USEC	TEMP. K	HN3	HN	N2	N2 (V=1)	CO2	CO2 MODE I	CO2 MODE II	GAIN
0.0	300.00	0.81D 18	0.0	0.0	0.0	0.40D 18	0.0	0.0	0.0
0.01	300.00	0.81D 18	0.14D 10	0.61D 06	0.61D 06	0.40D 18	0.38D 12	0.84D 05	0.0
0.51	300.00	0.81D 18	0.32D 13	0.83D 11	0.75D 11	0.40D 18	0.18D 14	0.26D 11	0.0
1.01	300.02	0.81D 18	0.12D 14	0.65D 12	0.55D 12	0.40D 18	0.33D 14	0.12D 12	0.0
1.51	300.05	0.81D 18	0.24D 14	0.22D 13	0.17D 13	0.40D 18	0.45D 14	0.34D 12	0.0
2.01	300.11	0.81D 18	0.38D 14	0.53D 13	0.39D 13	0.40D 18	0.56D 14	0.76D 12	0.0
2.51	300.19	0.81D 18	0.55D 14	0.10D 14	0.71D 13	0.40D 18	0.65D 14	0.15D 13	0.0
3.01	300.29	0.80D 18	0.74D 14	0.18D 14	0.12D 14	0.40D 18	0.72D 14	0.27D 13	0.0
3.51	300.43	0.80D 18	0.94D 14	0.28D 14	0.18D 14	0.40D 18	0.79D 14	0.46D 13	0.0
4.01	300.60	0.80D 18	0.11D 15	0.42D 14	0.25D 14	0.40D 18	0.84D 14	0.72D 13	0.0
4.51	300.81	0.80D 18	0.14D 15	0.59D 14	0.34D 14	0.40D 18	0.89D 14	0.11D 14	0.0
5.01	301.05	0.80D 18	0.16D 15	0.81D 14	0.44D 14	0.40D 18	0.93D 14	0.15D 14	0.0
5.51	301.32	0.80D 18	0.18D 15	0.11D 15	0.55D 14	0.40D 18	0.97D 14	0.21D 14	-0.00
6.01	301.63	0.80D 18	0.20D 15	0.14D 15	0.69D 14	0.40D 18	0.10D 15	0.28D 14	-0.00
6.51	301.98	0.80D 18	0.22D 15	0.17D 15	0.84D 14	0.40D 18	0.10D 15	0.37D 14	-0.00
7.01	302.37	0.80D 18	0.24D 15	0.21D 15	0.10D 15	0.40D 18	0.11D 15	0.48D 14	-0.00
7.51	302.79	0.80D 18	0.26D 15	0.26D 15	0.12D 15	0.40D 18	0.11D 15	0.60D 14	-0.00
8.01	303.26	0.80D 18	0.27D 15	0.31D 15	0.14D 15	0.40D 18	0.11D 15	0.75D 14	-0.00
8.51	303.76	0.80D 18	0.29D 15	0.37D 15	0.16D 15	0.40D 18	0.11D 15	0.92D 14	-0.00
9.01	304.31	0.80D 18	0.31D 15	0.44D 15	0.19D 15	0.40D 18	0.11D 15	0.11D 15	-0.00
9.51	304.90	0.80D 18	0.32D 15	0.51D 15	0.22D 15	0.40D 18	0.12D 15	0.13D 15	0.00
10.01	305.52	0.80D 18	0.33D 15	0.59D 15	0.25D 15	0.40D 18	0.12D 15	0.16D 15	0.00
10.51	306.19	0.80D 18	0.35D 15	0.68D 15	0.28D 15	0.40D 18	0.12D 15	0.19D 15	0.00
11.01	306.90	0.80D 18	0.36D 15	0.78D 15	0.32D 15	0.40D 18	0.12D 15	0.22D 15	0.00
11.51	307.66	0.80D 18	0.37D 15	0.89D 15	0.36D 15	0.40D 18	0.12D 15	0.26D 15	0.01
12.01	308.46	0.80D 18	0.38D 15	0.10D 16	0.41D 15	0.40D 18	0.13D 15	0.30D 15	0.01
12.51	309.31	0.80D 18	0.38D 15	0.11D 16	0.46D 15	0.40D 18	0.13D 15	0.35D 15	0.01
13.01	310.20	0.80D 18	0.39D 15	0.13D 16	0.52D 15	0.40D 18	0.13D 15	0.40D 15	0.01
13.51	311.14	0.80D 18	0.39D 15	0.14D 16	0.58D 15	0.40D 18	0.13D 15	0.46D 15	0.01
14.01	312.13	0.80D 18	0.40D 15	0.16D 16	0.65D 15	0.40D 18	0.14D 15	0.53D 15	0.02
14.51	313.17	0.80D 18	0.40D 15	0.18D 16	0.73D 15	0.40D 18	0.14D 15	0.60D 15	0.02
15.01	314.27	0.80D 18	0.40D 15	0.20D 16	0.81D 15	0.40D 18	0.14D 15	0.68D 15	0.02
15.51	315.42	0.80D 18	0.40D 15	0.22D 16	0.90D 15	0.40D 18	0.15D 15	0.77D 15	0.03
16.01	316.63	0.80D 18	0.40D 15	0.25D 16	0.99D 15	0.40D 18	0.15D 15	0.87D 15	0.03
16.51	317.90	0.80D 18	0.40D 15	0.28D 16	0.11D 16	0.40D 18	0.16D 15	0.98D 15	0.04
17.01	319.24	0.80D 18	0.40D 15	0.30D 16	0.12D 16	0.40D 18	0.16D 15	0.11D 16	0.04
17.51	320.64	0.79D 18	0.40D 15	0.34D 16	0.13D 16	0.40D 18	0.17D 15	0.12D 16	0.05
18.01	322.12	0.79D 18	0.40D 15	0.37D 16	0.15D 16	0.40D 18	0.18D 15	0.14D 16	0.06
18.51	323.67	0.79D 18	0.39D 15	0.41D 16	0.16D 16	0.40D 18	0.18D 15	0.15D 16	0.06
19.01	325.31	0.79D 18	0.39D 15	0.45D 16	0.18D 16	0.40D 18	0.19D 15	0.17D 16	0.07
19.51	327.04	0.79D 18	0.38D 15	0.49D 16	0.19D 16	0.40D 18	0.20D 15	0.19D 16	0.08
20.01	328.87	0.79D 18	0.38D 15	0.54D 16	0.21D 16	0.40D 18	0.21D 15	0.21D 16	0.09
20.51	330.81	0.79D 18	0.37D 15	0.60D 16	0.23D 16	0.40D 18	0.22D 15	0.23D 16	0.10
21.01	332.87	0.79D 18	0.37D 15	0.65D 16	0.25D 16	0.40D 18	0.23D 15	0.26D 16	0.12
21.51	335.07	0.79D 18	0.36D 15	0.72D 16	0.28D 16	0.40D 18	0.24D 15	0.28D 16	0.13
22.01	337.43	0.79D 18	0.36D 15	0.79D 16	0.30D 16	0.40D 18	0.25D 15	0.31D 16	0.14
22.51	339.98	0.79D 18	0.35D 15	0.86D 16	0.33D 16	0.40D 18	0.27D 15	0.34D 16	0.16
23.01	342.73	0.78D 18	0.35D 15	0.95D 16	0.36D 16	0.40D 18	0.28D 15	0.37D 16	0.18
23.51	345.75	0.78D 18	0.35D 15	0.10D 17	0.40D 16	0.40D 18	0.30D 15	0.41D 16	0.20
24.01	349.09	0.78D 18	0.35D 15	0.11D 17	0.44D 16	0.40D 18	0.32D 15	0.45D 16	0.22
24.51	352.83	0.78D 18	0.34D 15	0.13D 17	0.48D 16	0.40D 18	0.34D 15	0.49D 16	0.25
25.01	357.10	0.78D 18	0.35D 15	0.14D 17	0.54D 16	0.40D 18	0.36D 15	0.53D 16	0.27
25.51	362.10	0.77D 18	0.35D 15	0.16D 17	0.60D 16	0.40D 18	0.39D 15	0.59D 16	0.31
26.01	368.18	0.77D 18	0.36D 15	0.18D 17	0.69D 16	0.40D 18	0.42D 15	0.64D 16	0.34
26.51	376.00	0.77D 18	0.38D 15	0.20D 17	0.80D 16	0.40D 18	0.45D 15	0.71D 16	0.39
27.01	387.07	0.76D 18	0.43D 15	0.23D 17	0.98D 16	0.39D 18	0.49D 15	0.78D 16	0.44
27.51	406.24	0.75D 18	0.53D 15	0.29D 17	0.13D 17	0.39D 18	0.54D 15	0.88D 16	0.52
28.01	476.57	0.72D 18	0.99D 15	0.48D 17	0.28D 17	0.39D 18	0.64D 15	0.10D 17	0.68
28.02	483.77	0.72D 18	0.10D 16	0.50D 17	0.30D 17	0.39D 18	0.64D 15	0.10D 17	0.69
28.03	486.49	0.71D 18	0.11D 16	0.50D 17	0.30D 17	0.39D 18	0.65D 15	0.10D 17	0.70
28.03	489.38	0.71D 18	0.11D 16	0.51D 17	0.31D 17	0.39D 18	0.65D 15	0.10D 17	0.70
28.04	492.47	0.71D 18	0.11D 16	0.52D 17	0.32D 17	0.39D 18	0.65D 15	0.10D 17	0.70

TIME USEC	TEMP. K	HN3	HN	N2	N2 (V=1)	CO2	CO2 MODE I	CO2 MODE II	GAIN
28.11	594.67	0.66D 18	0.16D 16	0.78D 17	0.56D 17	0.39D 18	0.70D 15	0.11D 17	0.78
28.11	616.23	0.65D 18	0.17D 16	0.83D 17	0.61D 17	0.39D 18	0.70D 15	0.11D 17	0.78
28.12	645.78	0.64D 18	0.19D 16	0.90D 17	0.68D 17	0.39D 18	0.71D 15	0.11D 17	0.79
28.12	690.01	0.61D 18	0.20D 16	0.10D 18	0.79D 17	0.39D 18	0.72D 15	0.11D 17	0.79
28.13	766.96	0.58D 18	0.23D 16	0.12D 18	0.98D 17	0.39D 18	0.73D 15	0.11D 17	0.78
28.13	948.05	0.49D 18	0.28D 16	0.17D 18	0.14D 18	0.39D 18	0.76D 15	0.11D 17	0.73
28.14	1596.58	0.16D 18	0.44D 16	0.33D 18	0.31D 18	0.39D 18	0.86D 15	0.11D 17	0.52
28.14	1898.31	0.19D 16	0.50D 16	0.41D 18	0.38D 18	0.39D 18	0.12D 16	0.12D 17	0.46
28.15	1902.04	0.14D 14	0.50D 16	0.41D 18	0.38D 18	0.39D 18	0.15D 16	0.13D 17	0.48
28.15	1902.15	0.10D 12	0.49D 16	0.41D 18	0.38D 18	0.39D 18	0.19D 16	0.14D 17	0.51
28.17	1902.38	0.0	0.48D 16	0.42D 18	0.37D 18	0.38D 18	0.29D 16	0.17D 17	0.53
28.67	1906.85	0.0	0.29D 16	0.52D 18	0.22D 18	0.35D 18	0.14D 17	0.42D 17	1.21
29.17	1908.76	0.0	0.21D 16	0.57D 18	0.16D 18	0.35D 18	0.13D 17	0.35D 17	0.93
29.67	1909.82	0.0	0.16D 16	0.62D 18	0.13D 18	0.36D 18	0.12D 17	0.27D 17	0.66
30.17	1910.50	0.0	0.13D 16	0.65D 18	0.11D 18	0.37D 18	0.10D 17	0.22D 17	0.50
30.67	1910.96	0.0	0.11D 16	0.69D 18	0.11D 18	0.37D 18	0.99D 16	0.20D 17	0.41
31.17	1911.30	0.0	0.96D 15	0.72D 18	0.11D 18	0.37D 18	0.97D 16	0.19D 17	0.38
31.67	1911.57	0.0	0.85D 15	0.75D 18	0.11D 18	0.37D 18	0.97D 16	0.19D 17	0.38
32.17	1911.77	0.0	0.76D 15	0.79D 18	0.12D 18	0.37D 18	0.98D 16	0.19D 17	0.39
32.67	1911.94	0.0	0.69D 15	0.83D 18	0.12D 18	0.37D 18	0.99D 16	0.20D 17	0.41
33.17	1912.08	0.0	0.63D 15	0.86D 18	0.12D 18	0.37D 18	0.10D 17	0.20D 17	0.41
33.67	1912.19	0.0	0.58D 15	0.90D 18	0.12D 18	0.37D 18	0.99D 16	0.19D 17	0.39
34.17	1912.29	0.0	0.53D 15	0.94D 18	0.12D 18	0.37D 18	0.98D 16	0.18D 17	0.36
34.67	1912.37	0.0	0.50D 15	0.97D 18	0.11D 18	0.38D 18	0.96D 16	0.17D 17	0.32
35.17	1912.45	0.0	0.46D 15	0.10D 19	0.10D 18	0.38D 18	0.93D 16	0.16D 17	0.28
35.67	1912.51	0.0	0.44D 15	0.10D 19	0.92D 17	0.38D 18	0.90D 16	0.14D 17	0.23
36.17	1912.57	0.0	0.41D 15	0.11D 19	0.82D 17	0.38D 18	0.87D 16	0.13D 17	0.18
36.67	1912.62	0.0	0.39D 15	0.11D 19	0.73D 17	0.38D 18	0.84D 16	0.11D 17	0.13
37.17	1912.67	0.0	0.37D 15	0.11D 19	0.64D 17	0.38D 18	0.81D 16	0.10D 17	0.09
37.67	1912.71	0.0	0.35D 15	0.11D 19	0.56D 17	0.39D 18	0.78D 16	0.88D 16	0.04
38.17	1912.75	0.0	0.33D 15	0.11D 19	0.48D 17	0.39D 18	0.75D 16	0.77D 16	0.01
38.67	1912.78	0.0	0.32D 15	0.11D 19	0.41D 17	0.39D 18	0.73D 16	0.67D 16	-0.03
39.17	1912.81	0.0	0.31D 15	0.11D 19	0.36D 17	0.39D 18	0.71D 16	0.58D 16	-0.05
39.67	1912.84	0.0	0.29D 15	0.12D 19	0.30D 17	0.39D 18	0.69D 16	0.50D 16	-0.08
40.17	1912.87	0.0	0.28D 15	0.12D 19	0.26D 17	0.39D 18	0.67D 16	0.43D 16	-0.10
40.67	1912.89	0.0	0.27D 15	0.12D 19	0.22D 17	0.39D 18	0.66D 16	0.37D 16	-0.12
41.17	1912.92	0.0	0.26D 15	0.12D 19	0.19D 17	0.39D 18	0.65D 16	0.32D 16	-0.14
41.67	1912.94	0.0	0.25D 15	0.12D 19	0.16D 17	0.39D 18	0.64D 16	0.28D 16	-0.15
42.17	1912.96	0.0	0.24D 15	0.12D 19	0.14D 17	0.39D 18	0.63D 16	0.25D 16	-0.16
42.67	1912.97	0.0	0.24D 15	0.12D 19	0.12D 17	0.39D 18	0.62D 16	0.22D 16	-0.17
43.17	1912.99	0.0	0.23D 15	0.12D 19	0.10D 17	0.39D 18	0.62D 16	0.19D 16	-0.18
43.67	1913.01	0.0	0.22D 15	0.12D 19	0.88D 16	0.39D 18	0.61D 16	0.17D 16	-0.19
44.17	1913.02	0.0	0.21D 15	0.12D 19	0.77D 16	0.39D 18	0.61D 16	0.15D 16	-0.19
44.67	1913.04	0.0	0.21D 15	0.12D 19	0.67D 16	0.40D 18	0.61D 16	0.14D 16	-0.20
45.17	1913.05	0.0	0.20D 15	0.12D 19	0.58D 16	0.40D 18	0.60D 16	0.13D 16	-0.20
45.67	1913.06	0.0	0.20D 15	0.12D 19	0.51D 16	0.40D 18	0.60D 16	0.12D 16	-0.20
46.17	1913.08	0.0	0.19D 15	0.12D 19	0.46D 16	0.40D 18	0.60D 16	0.11D 16	-0.21
46.67	1913.09	0.0	0.19D 15	0.12D 19	0.41D 16	0.40D 18	0.60D 16	0.99D 15	-0.21
47.17	1913.10	0.0	0.18D 15	0.12D 19	0.37D 16	0.40D 18	0.59D 16	0.93D 15	-0.21
47.67	1913.11	0.0	0.18D 15	0.12D 19	0.33D 16	0.40D 18	0.59D 16	0.88D 15	-0.21
48.17	1913.12	0.0	0.17D 15	0.12D 19	0.31D 16	0.40D 18	0.59D 16	0.84D 15	-0.21
48.67	1913.13	0.0	0.17D 15	0.12D 19	0.28D 16	0.40D 18	0.59D 16	0.80D 15	-0.21
49.17	1913.14	0.0	0.17D 15	0.12D 19	0.26D 16	0.40D 18	0.59D 16	0.77D 15	-0.22
49.67	1913.15	0.0	0.16D 15	0.12D 19	0.25D 16	0.40D 18	0.59D 16	0.75D 15	-0.22
50.17	1913.15	0.0	0.16D 15	0.12D 19	0.23D 16	0.40D 18	0.59D 16	0.73D 15	-0.22
50.67	1913.16	0.0	0.15D 15	0.12D 19	0.22D 16	0.40D 18	0.59D 16	0.71D 15	-0.22

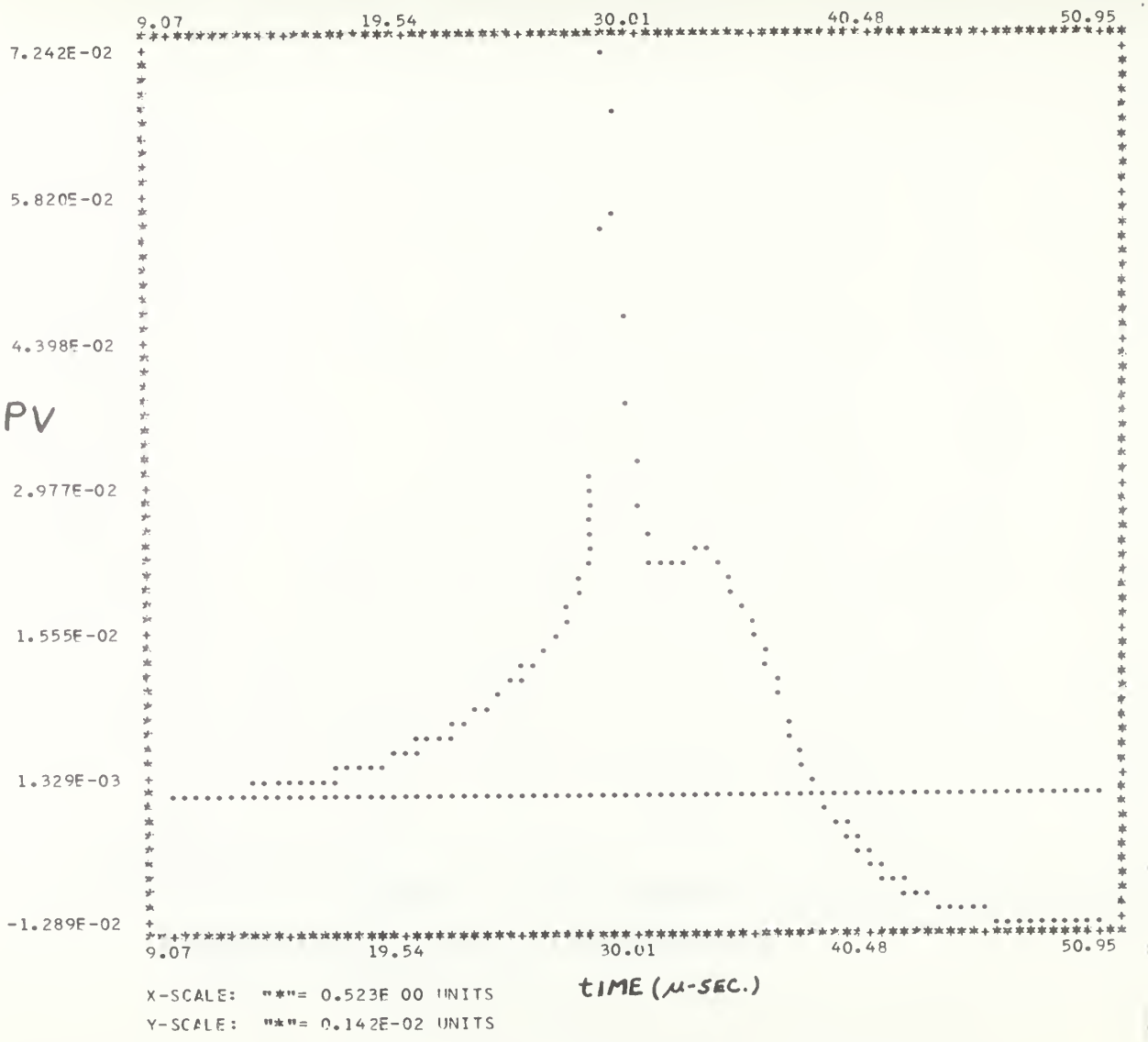

POPULATION INVERSION BETWEEN MODES I AND II OF CO_2

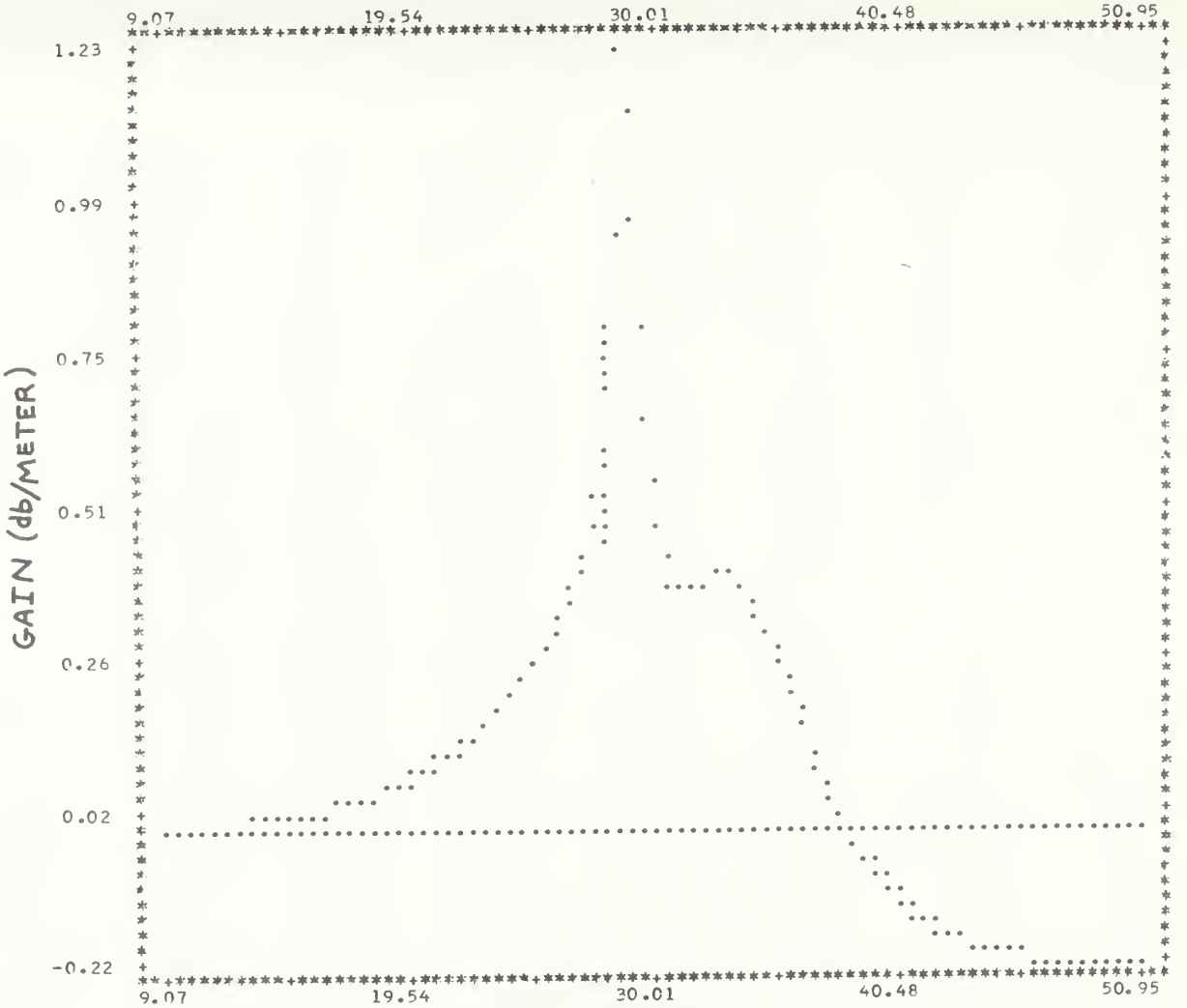

THE LASER GAIN PRODUCED IN CO_2 FOR λ= 10.6 microns.

BIBLIOGRAPHY

1. Waddington, T. C., "Spontaneous Ignition of Gaseous Hydrogen Azide," Nature, v. 179, p. 576-577, 16 March 1957.

2. Konar, R. S., Matsumoto, S., Darwent, B. De B., "Photochemical Decomposition of Gaseous Hydrogen Azide," Canadian Journal of Chemistry, v. 49, p. 1698, 12 June 1970.

3. Okabe, Hideo, "Photodissociation of HN_3 in the Vacuum-Ultraviolet Production and Reactivity of Electronically Excited NH," The Journal of Chemical Physics, v. 49, p. 2726-2733, 15 September 1968.

4. Thrush, B. A., "The Detection of Free Radicals in the High Intensity Photolysis of Hydrogen Azide," Proceedings of the Royal Society A, v. 235, p. 143-147, 1956.

5. Beckman, A. O., and Dickinson, R. G., "The Quantum Yield in the Photochemical Decomposition of Hydrogen Azide," Journal of the American Chemical Society, v. 52, p. 124-131, 1956.

6. Becker, E. D., Pimentel, G. C., Van Thiel, M., "Matrix Isolation Studies: Infrared Spectra of Intermediate Species in the Photolysis of Hydrazoic Acid," The Journal of Chemical Physics, v. 26, p. 145-149, January 1957.

7. Papazian, H. A., "Nitrogen Chained Compounds as Intermediates in the Photolysis of Solid HN," The Journal of Chemical Physics, v. 32, p. 456-460, February 1970.

8. Voronkov, V. G., and Rozenberg, A. S., "Explosive Properties of Mixtures of Gaseous Hydrazoic Acid with Inorganic Diluents," Academy of Sciences, U.S.S.R. Proceedings, Chemistry Section, v. 177, p. 1103-1106, 1967.

9. Voronkov, V. G., and Rozenberg, A. S., "Ignition of Hydrazoic Acid with a Series of Inorganic Diluents," Russian Journal of Physical Chemistry, v. 43, p. 1333-1335, 1969.

10. Voronkov, V. G., Rozenberg, A. S., and Arsen'ev, Yu. N., "Ignition of Gaseous Mixtures of Hydrogen Azide and Methane," Russian Journal of Physical Chemistry, v. 44, 1. 1165-1166, 1970.

11. Basov, N. G., Gromov, V. V., Koshelev, E. L., Markin, E. P., and Oraevskii, A. N., "Emission Stimulated by Explosion of HN_3 in CO_2," Zh. Tekh. Fiz. (Soviet Physics - Technical Physics), v. 38, p. 2031, 1968, v. 13, p. 1630, 1969.

12. Dzhidzhoev, M. S., Pimenov, M. I., Platonenko, V. G., Filippov, Yu. V., and Khokhlov, R. V., "Creation of a Population Inversion in Polyatomic Molecules Through the Energy of Chemical Reactions," Soviet Physics JetP, v. 30, p. 225-229, February 1970.

13. Cornell, D. W., Berry, R. S., and Lwowski, W., Journal American Chemical Society, v. 88, p. 544, 1966.

14. Welge, K. H., "Formation of $NH(c^1\Pi)$ and $NH(A^3\Pi_i)$ in the Vacuum-uv Photolysis of HN_3," Journal of Chemical Physics, v. 45, p. 4373-4374, 1966.

15. Welge, K. H., "Formation of $N_2(A^3 \sum_g^+)$ and $N(^2D, ^2P)$ by Photodissociation of HN_3 and N_2O and Their Reactions with NO and N_2O," The Journal of Chemical Physics, v. 45, p. 166-170, 1966.

16. Stuhl, F., "Dissertation," The University of Bonn, Bonn, Germany, 1966.

17. Konar, R. S. and Darwent, B. De B., Canadian Journal of Chemistry, v. 48, 1970.

18. Lengyel, B. A., Introduction to Laser Physics, p. 40-42, John Wiley and Son, Inc., New York, 1966.

19. Corneil, P. H., The HCL Chemical Laser, Ph.D Thesis, University of California, Berkeley, 1967.

20. Platt, G. L., Gas Kinetics, Wiley, 1969.

21. Semenov, N. N., and Shilov, A. E., "On the Role of Excited Particles in Branched Chain Reactions," Kinetics and Catalysis, v. 6, p. 1-11, 1965.

22. Clarke, J. F., and McChesney, M., The Dynamics of Real Gases, Butterworths, 1964.

23. Airey, J. R., "Cl + HBr Pulsed Chemical Laser: A Theoretical and Experimental Study," The Journal of Chemical Physics, v. 52, p. 156-167, January 1970.

24. Naval Ordnance Laboratory, NOLTR 71-116, Population Inversions in an Expanding Gas: Theory and Experiment, J. D. Anderson, Jr., R. L. Humphrey, J. S. Vamos, M. J. Plummer and R. E. Jensen, 28 June 1971.

25. Tyte, D. C., Advances in Quantum Electronics, v. 1, p. 129-157, Academic Press, 1970.

26. Patel, C. K. N., "Selective Excitation Through Vibrational Energy Transfer and Optical Laser Action in N_2 - CO_2," Physical Review Letters, v. 13, p. 811-813, 23 November 1964.

27. Moore, C. B., Wood, R. E., Hu, B. L., and Yardley, J. T., "Vibrational Energy Transfer in CO_2 Lasers," The Journal of Chemical Physics, v. 46, p. 4222-4231, 1 June 1961.

28. Rapp, D., and Englander-Golden, P., "Resonant and Near-Resonant Vibrational-Vibrational Energy Transfer Between Molecules in Collisions," The Journal of Chemical Physics, v. 40, p. 573-576, 15 January 1964.

29. Taylor, R. L., Bitterman, S., "Survey of Vibrational Relaxation Data for Processes Important in the CO_2-N_2 Laser System," Review of Modern Physics, v. 41, p. 26-45, January 1969.

30. Markiewicz, J. P., and Emmett, J. L., "Design of Flashlamp Driving Circuits," IEEE Journal of Quantum Electronics, v. QE-2, p. 707-711, November 1966.

31. Oral communication with Professor Rowell, Department of Chemistry, U. S. Naval Postgraduate School, Monterey, California.

32. Deschamps, G. A., and Mast, P. E., "Proceedings of the Symposium on Quasi-Optics," p. 379, Polytechnic Press, 1964.

33. Bahn, G. S., Reaction Rate Compilation for the H-O-N System, v. 5, Gordon and Breach, 1967.

INITIAL DISTRIBUTION LIST

		No. Copies
1.	Defense Documentation Center Cameron Station Alexandria, Virginia 22314	2
2.	Library, Code 0212 Naval Postgraduate School Monterey, California 93940	2
3.	Professor R. W. Bell, Code 57Be Chairman, Department of Aeronautics Naval Postgraduate School Monterey, California 93940	1
4.	Professor D. J. Collins, Code 057 Department of Aeronautics Naval Postgraduate School Monterey, California 93940	1
5.	LT Francis K. Helmsin, USN 101 Malloway Lane Monterey, California 93940	1

Security Classification

DOCUMENT CONTROL DATA - R & D

(Security classification of title, body of abstract and indexing annotation must be entered when the overall report is classified)

1. ORIGINATING ACTIVITY *(Corporate author)*
Naval Postgraduate School
Monterey, California 93940

2a. REPORT SECURITY CLASSIFICATION
Unclassified

2b. GROUP

3 REPORT TITLE
The $HN_3 + CO_2$ Laser: An Analytical and Experimental Investigation

4 DESCRIPTIVE NOTES *(Type of report and, inclusive dates)*
Master's Thesis (March 1972

5. AUTHOR(S) *(First name, middle initial, last name)*
Francis Kenneth Helmsin

6. REPORT DATE	7a. TOTAL NO. OF PAGES	7b. NO. OF REFS
March 1972	79	33

8a. CONTRACT OR GRANT NO.	9a. ORIGINATOR'S REPORT NUMBER(S)
b. PROJECT NO.	
c.	9b. OTHER REPORT NO(S) *(Any other numbers that may be assigned this report)*
d.	

10. DISTRIBUTION STATEMENT
Approved for public release; distribution unlimited

11. SUPPLEMENTARY NOTES	12. SPONSORING MILITARY ACTIVITY
	Naval Postgraduate School Monterey, California 93940

13. ABSTRACT

One of the most important methods of obtaining laser action, both from a technological and scientific viewpoint, is the chemically-pumped laser. The $HN_3 + CO_2$ chemical laser has been modeled and an experimental investigation conducted to determine the existence of laser action. The analytical model has been used to predict the expected population inversion and laser gain for a range of pressures and various additives. The experimental investigation conducted for comparison with the model did not result in laser action. The increase in pressure for the mixtures investigated indicates the occurrence of an explosion. The lack of detection of laser action has been attributed to difficulties with alignment of the optical system and to signal noise associated with the flash circuit.

14 KEY WORDS	LINK A		LINK B		LINK C	
	ROLE	WT	ROLE	WT	ROLE	WT
Laser						
Laser Gain						
Explosive						
Hydrogen Azide						
Flash Photolysis						
Chemical Laser						


6
7
8
9
10
7
8
9
10
11
70
500


OREGON
RULE
CO.
U.S.A.
60